SEG Special Publications, no. 21, pp. 237–269

Chapter 11

Fault-Controlled Fluid Flow Within Extensional Basins and Its Implications for Sedimentary Rock-Hosted Mineral Deposits

John J. Walsh,[1,†] Koen Torremans,[1] John Güven,[1] Roisin Kyne,[1] John Conneally,[1] and Chris Bonson[2]

[1] *Irish Centre for Research in Applied Geosciences, Fault Analysis Group, School of Earth Sciences, University College Dublin, Belfield, Dublin 4, Ireland*

[2] *Tektonik Consulting Ltd, Abergavenny, Monmouthshire, United Kingdom*

Abstract

Normal faults commonly represent one of the principal controls on the origin and formation of sedimentary rock-hosted mineral deposits. Their presence within rift basins has a profound effect on fluid flow, with their impact ranging from acting as barriers, causing pressure compartmentalization of basinal pore fluids, to forming conduits for up-fault fluid flow. Despite their established importance in controlling the migration and trapping of mineralizing fluids, we have yet to adequately reconcile this duality of flow behavior and its impact on mineral flow systems within basinal sequences from a semiquantitative to quantitative perspective. Combining insights and models derived from earthquake, hydrocarbon, and mineral studies, the principal processes and models for fault-related fluid flow within sedimentary basins are reviewed and a unified conceptual model defined for their role in mineral systems. We illustrate associated concepts with case studies from Irish-type Zn-Pb deposits, sedimentary rock-hosted Cu deposits, and active sedimentary basins. We show that faults can actively affect fluid flow by a variety of associated processes, including seismic pumping and pulsing, or can provide pathways for the upward flow of overpressured fluids or the downward sinking of heavy brines. Associated models support the generation of crustal-scale convective flow systems that underpin the formation of major mineral provinces and provide a basis for differences in the flow behavior of faults, depending on a variety of factors such as fault zone complexities, host-rock properties, deformation conditions, and pressure drives. Flow heterogeneity along faults provides a basis for the thoroughly 3D flow systems that localize fluid flow and lead to the formation of mineral deposits.

Introduction

Faults represent one of the principal controls on fluid flow within the subsurface, acting either as conduits or barriers within a variety of flow regimes, including groundwater, hydrocarbon, and minerals systems (e.g., Muir-Wood and King, 1993; Cox et al., 2001; Sibson, 2001; Manzocchi et al., 2010). Over the past five decades, a much better understanding has been developed of (1) the conductive nature of faults and fractures within otherwise poor aquifers/reservoirs, such as limestone and basement, (2) fluid flow within faulted siliciclastic sequences, and (3) the general impact of fault conduits and sealing within sedimentary basins and petroleum provinces (Fisher and Knipe, 2001; Nelson, 2001; Bence and Person, 2006; Manzocchi et al., 2010). Associated studies have benefitted from the acquisition of a broad range of fluid flow data and the currently active nature of flow, facilitating the definition and parameterization of numerical flow models, and permitting the rigorous testing of the flow system and the development of improved predictive capabilities (e.g., Jolley et al., 2007a). For example, the incorporation of faults as baffles or barriers within flow simulation models of clastic hydrocarbon reservoirs is now relatively routine, with existing methods providing a much-improved basis for history matching and production forecasting (Manzocchi et al., 1999; Jolley et al., 2007b). Significant advances have also been made for modeling the conductive nature of fractures within fractured reservoirs, with a variety of tools permitting history matching with reservoir production. An emerging view is that conductive fracture fluid flow is very heterogeneous and can be unpredictable, particularly for fault/fracture systems which have scale-invariant properties (e.g., with geometric characteristics covering a broad range of scales; Odling et al., 1999; Nelson, 2001). This challenge can partly be circumvented by a variety of engineering-based innovations, such as well testing, reservoir stimulation, and horizontal drilling. Similar heterogeneous flow characteristics have been attributed to hydrothermal flow systems within low-porosity and -permeability host rocks, where fracture-controlled fluid flow favors localized ore deposits (Cox, 2005), oftentimes adjacent to structural complexities on faults (Newhouse, 1942; Sibson, 2000; Cox et al., 2001).

Previous structural geology research has concentrated on fault- and shear zone-related vein deposits, typically developed within metamorphic basement rocks and in orogenic rather than sedimentary basin settings (e.g., Sibson, 1987, 1996; Sibson and Scott, 1998; Cox, 2005). This emphasis is not surprising given the economic importance of structurally controlled vein deposits, in which vein systems represent both the conduits and host for mineralization. In this paper, we review the principal processes and models for fault-related fluid flow within extensional basins and their implications for the nature and origin of sedimentary rock-hosted mineral deposits, also referred to as sediment-hosted mineral deposits. Drawing heavily from previous work on earthquake, hydrocarbon, and mineral deposit systems, we illustrate the variety of roles faults play in the genesis of associated mineral provinces and

† Corresponding author: e-mail, john.walsh@ucd.ie

doi: 10.5382/sp.21.11; 33 p.

the formation of individual deposits. Illustrating related concepts with evidence from active basins and from Irish-type Zn-Pb deposits and sedimentary rock-hosted Cu deposits, we address a selection of associated fundamental issues, including the principal drivers for basinal fluid flow, the factors controlling fault-related fluid flow, the nature of fault zone complexity and associated flow localization, and the impact of faults on sedimentary rock-hosted mineral deposits.

The Essential Ingredients of Sedimentary Rock-Hosted Mineral Provinces

Sedimentary basins arising from crustal extension are marked by crustal thinning and associated basinal subsidence, together with upwelling of underlying lithosphere and an associated increase in geothermal gradient (Fig. 1). At upper crustal levels, within the seismogenic zone, extension is accommodated predominantly by brittle faulting that exercises a major control on basinal accommodation space and the geometry and nature of the basin fill. At greater depths, deformation becomes more ductile (plastic), with individual faults extending into underlying shear zones and distributed pure shear (e.g., Roberts and Yielding, 1994; Sibson, 2000). Whereas details of the sedimentary sequences differ between basins, they commonly have two generic characteristics: the increased prevalence of evaporitic units toward the base of the sequence and a progressive upward increase in shale. These features reflect ongoing basin subsidence, which is marked by early lacustrine and potential red-bed facies, with shallow marine incursions, followed by gradual deepening toward deeper-water sedimentary facies. These changes typically accompany the transition from synrift sequences into postrift sequences and, together with faulting, allow the development of a hydrologically closed basinal architecture as a backdrop to the generation of sedimentary rock-hosted mineral deposits and provinces (Pirajno, 2000; Selley et al., 2005; Koziy et al., 2009; Hitzman et al., 2010).

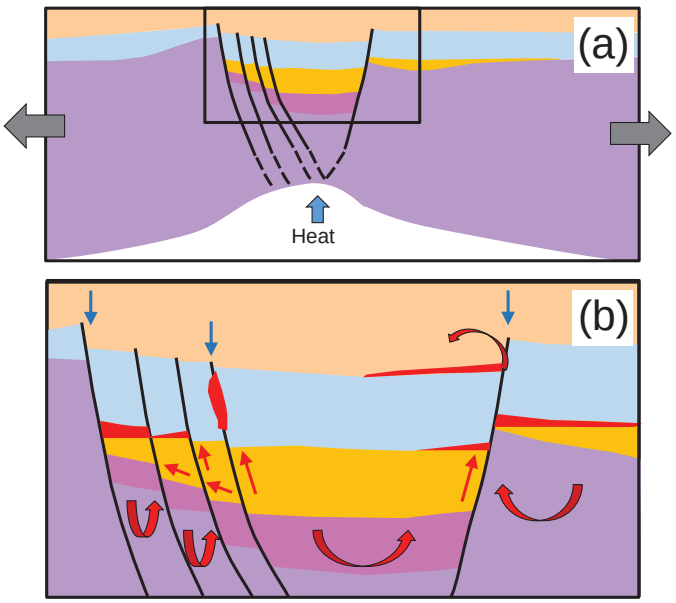

Fig. 1. (a, b) Schematic diagrams of the structure and flow paths of an extensional sedimentary basin (after Hitzman et al., 2010). Convective flow shown in (b) arises from the downflow of brines (blue arrows) or their remobilization from basinal red-bed facies (red arrows) at the base of the synrift sequence, combined with the upward flow of hot mineralizing fluids arising from the elevated geothermal gradients associated with crustal thinning.

Previous studies on sedimentary rock-hosted mineral deposits (e.g., Leach et al., 2005; Hitzman et al., 2010; Wilkinson and Hitzman, 2015) have identified the following key elements of associated mineral provinces: (1) the availability of brines, from both evaporitic and marine sequences, which form mineralizing fluids, (2) suitable sedimentary or basement rocks providing the metal source for scavenging fluids, (3) a source of sulfur, (4) elevated heat, which causes buoyancy-driven fluid flow of saline brines, (5) the prevalence of faults that are the key pathways for upward and downward flow, with the emergence of convective flow providing the means of generating a sustained flow system, and (6) the presence of appropriate traps and the right chemical and physical factors to cause precipitation from mineralizing fluids, either by pore-filling or replacive processes, within stratabound/stratiform and/or crosscutting bodies. In this paper, we concentrate on the last two requirements relating to faulting and their crucial role in basinal fluid flow and the formation of mineral deposits. Before we consider details of fault-related impacts, we first consider some generic issues relating to fluid flow within different host rocks and to the hydrodynamics of sedimentary basins, irrespective of their mineral prospectivity.

The Nature of Flow Within Sediments and the Importance of Faults

The nature of fluid flow within host rocks provides the essential backdrop to fault-related fluid flow and the formation of associated mineral deposits. From a flow perspective, however, it is useful to make a clear distinction between the two most common end-member host-rock sequences within basins: siliciclastic rocks and carbonates.

Porous siliciclastic host rocks

Sedimentary rocks within siliciclastic sequences are commonly represented in flow models using averaged hydraulic properties, such as porosity and permeability. Flow through individual sandstone or shale units can be approximated by the standard expression for Darcy flow,

$$Q = -\frac{\kappa A\,(p\mathrm{b} - p\mathrm{a})}{\mu \mathrm{L}}, \qquad (1)$$

where the flow rate (Q, m^3/s) through a cross-sectional area (A, m^2) in a porous medium relates to the permeability of the rock (κ, m^2), the viscosity of the fluid (μ, Pa.s), and the pressure drop ($p_b - p_a$) over a given distance (L, m). Because of the relatively homogeneous nature of the host rocks, fluid flow within porous media can be predictable and well approximated in numerical flow simulations (Manzocchi et al., 2008a). In situ measurements from aquifers and hydrocarbon reservoirs highlight the systematic nature of fluid flow, with well-behaved flow fronts. At the same time, however, the compactive and cataclastic effect of faulting in siliciclastic rocks will create lower-porosity/-permeability fault rocks that can be barriers to across-fault flow between otherwise porous and permeable host rocks (e.g., sandstones; Fisher and Knipe, 2001). Even then, the nature of flow across faults can be averaged (i.e., upscaled) at scales greater than the fault rock heterogeneity

(Manzocchi et al., 2008a, b). Because of the relatively low effective vertical permeabilities of mixed clastic sequences (i.e., K_v), the very same faults that act as barriers for across-fault flow can represent conduits for upward along-fault flow, providing a conduit-barrier system to fluid flow (e.g., Bence and Person, 2006; Jolley et al., 2007a; Manzocchi et al., 2010). Although predictive methods for fault sealing within siliciclastic sequences are now routinely used within the hydrocarbon industry (Manzocchi et al., 2010), the nature of conductive fluid flow along very heterogeneous fault zones is much more difficult to model, an issue we consider later in this paper.

Low-porosity host rocks

Flow within otherwise low porosity and permeability carbonate/limestone and basement is entirely controlled by associated fault/fracture porosity and permeability (Nelson, 2001). In these circumstances, faults will generate permeable fault rocks and act exclusively as conduits to fluid flow until they become sealed by cementation. The heterogeneous nature of flow within reservoirs dominated by fracture-controlled flow (e.g., within basement rocks and limestones) is well established (Nelson, 2001), and similar behavior is seen within equivalent groundwater and mineral deposit systems (Cox, 2005; Neuman, 2008). The complex nature of fracture-controlled flow is attributed to a variety of factors, including the connectivity of fractures, variable aperture distributions, stress sensitivity, and mechanical flow coupling (Zhang and Sanderson, 1996; Nelson, 2001). The bulk permeability of a fracture system comprising randomly distributed fractures can be approximated by the equation

$$k = (\pi/120) \cdot f a^3 l^2/s^3, \quad (2)$$

where a is the mean fracture aperture, l is the mean fracture length, s is the mean fracture spacing, and connectivity f is between 0 and 1 (Guéguen and Dienes, 1989). This equation reflects the "cubic flow law," in which flow varies with the cube of aperture or openings along faults/fractures. It also shows the strong dependency of fracture-related fluid flow on other properties such as fracture spacing or length, which in many systems have scale-invariant or power-law scaling themselves (e.g., with geometric characteristics covering a broad range of scales; Walsh et al., 1991; Yielding et al., 1992). These relationships demonstrate that, even within a fault/fracture system which is macroscopically connected, extreme flow heterogeneity will arise from the very nonlinear relationship between fracture aperture and flow rate, and the heterogeneous nature of fault/fracture distributions and connectivity (Cox, 2005; Neuman, 2008). Such behavior is typical of conductive fault/fracture systems in the hydrocarbon industry—systems that are notoriously difficult to predict (Nelson, 2001). It is this flow-localizing characteristic of conductive faults that makes fault-related mineral deposits what they are: rock volumes marking the passage and trapping of large volumes of fluids, whether the host rock is a porous sediment, a fractured aquifer, or an easily replaced reservoir.

What Are the Main Drives for Basinal Fluid Flow?

The geometric configuration of faults provides the essential backdrop for fluid flow within sedimentary basins. Fault systems comprise arrays of normal faults of different size (lengths and maximum displacements), which together accommodate crustal thinning and subsidence. They have a major impact on the burial, thermal, and structural evolution of basins, all of which are the prime drivers of fluid flow.

Fault systems are highly interactive from earthquake through to geologic time scales, always displaying the conservation and transfer of displacement between faults, despite the discontinuous nature of individual structures and subbasins (Figs. 2, 3; Walsh and Watterson, 1991). Associated stress- and fluid-related interactions are strongly linked to displacements accommodated by earthquake events and/or aseismic creep, which provide another means of driving fluid movement during basin development, an issue we will address later. First, however, we will consider how other processes contribute to basinal fluid flow and how faults passively impact flow regimes, mainly in the context of the North Sea basin, which is in its postrift phase and is therefore not complicated by active faulting and earthquake-related drives. After that, we outline how active tectonism drives fluid flow and how fault zone heterogeneity and structural complexity affect fault-related fluid flow.

Basinal pore fluid pressures

One of the principal drivers for basinal fluid flow arises from disequilibrium compaction, in which sediment loading leads to progressive porosity loss and the closing of pore-throat spaces (Osborne and Swarbrick, 1998; Swarbrick et al., 2002). Other factors, including mineral transformations and cementation, hydrocarbon generation, and aquathermal expansion, can contribute to overpressuring and fluid expansion but are generally considered to be subordinate to mechanical compaction (Swarbrick et al., 2002). Together, these processes are responsible for a buildup of pore-fluid pressures with depth, from hydrostatic conditions, where pore fluids are open to the surface, to progressively higher pore-fluid pressures approaching lithostatic pressures, whereby the interstitial pore fluids progressively support the rock column. The degree of overpressuring is quantified using the pore-fluid pressure ratio, λ, which ranges from 0.4 to 1.0, for hydrostatic through to lithostatic conditions. Analysis of present-day basins shows that the depth at which pore fluids increase, referred to as the isolation (or fluid retention) depth, is controlled by a variety of factors, including sediment porosity and permeability, sedimentation (and therefore loading) rate, and basin configuration (Fig. 4; Swarbrick et al., 2002). Because permeability controls the rate of fluid expulsion, isolation depths are typically shallower in less permeable mudrocks than within more permeable siltstones and sandstones, and are also shallower for high sedimentation rates. Pressure data from the North Sea indicate isolation depths generally between 0.7 and 2.5 km with pressures increasing to λ values of 0.8 to 0.9 at depths of approximately 5 km and greater (Fig. 4). Very high fluid pressures will lead to the valving of fluids by faults, a mechanically driven response even in the absence of active crustal extension. Individual pore-fluid pressure profiles highlight their lithological dependence and variability, with pressure increases commonly coinciding with the boundaries of impermeable (i.e., sealing) facies and underlying aquifers/reservoirs (Fig. 4). Whereas pore pressure profiles provide a basis for the hydrodynamics of a basin, with lateral and

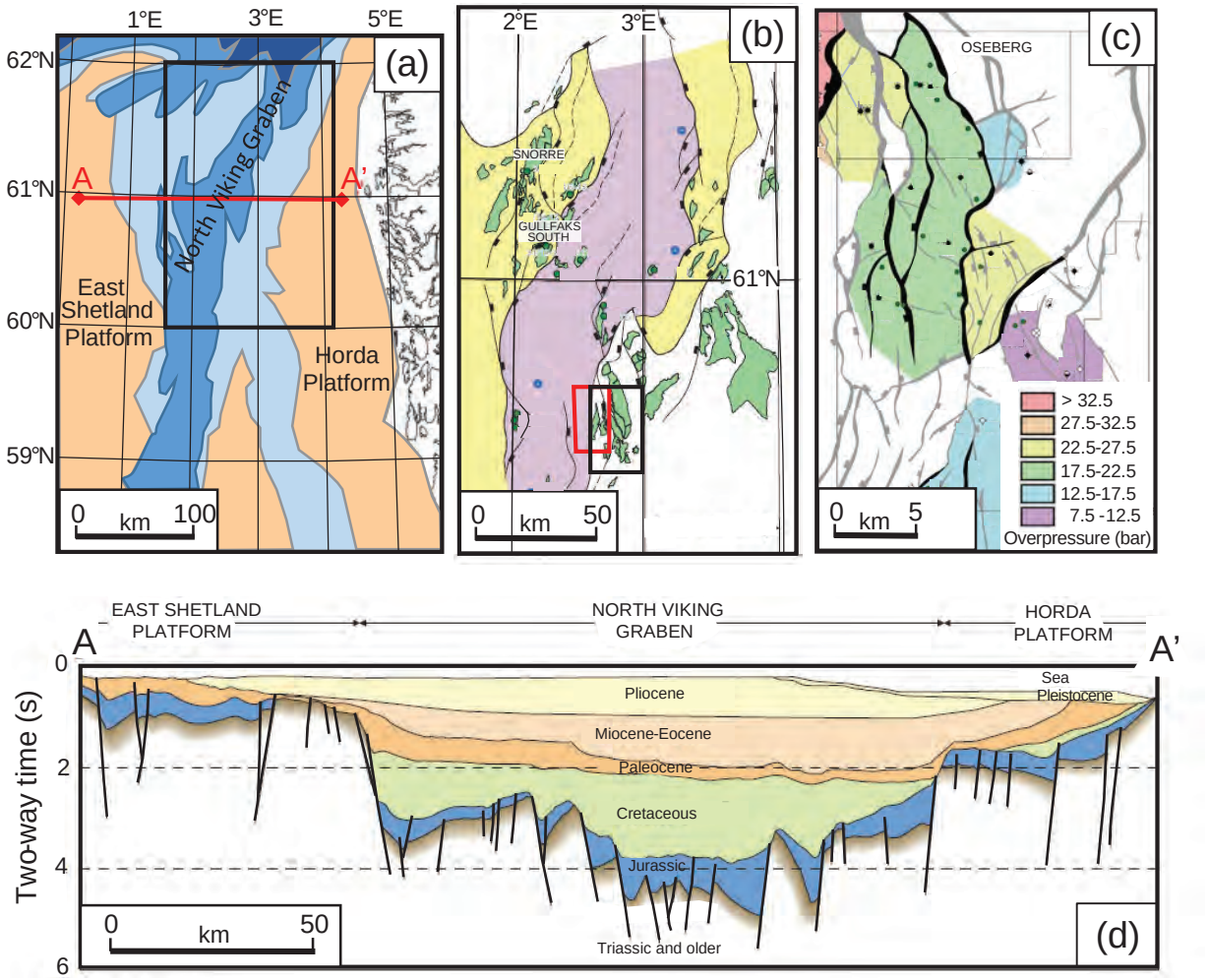

Fig. 2. Structure- and fault-controlled fluid compartmentalization in the North Viking graben (modified from Nordgård Bolås and Hermanrud, 2003). (a) Map of North Viking graben showing the location of map (black rectangle) in (b) and the cross section A-A' in (d). Ultradeep (dark blue), deep basins/terraces (medium blue), and shelf areas (light blue) are distinguished from platform highs (beige). (b) Map showing pore-fluid pressures in which overpressures either exceed (purple) or are less than (yellow) 200 bars; white is normally pressured. Black rectangle is the location of map in (c), and red rectangle is the location of 3D model in Figure 6. (c) Pore fluid overpressure (bars) for the Tarbert Reservoir in the Tune area (Lothe et al., 2006). (d) Cross section of the North Viking graben. Depth is in two-way travel time (s) and, while the velocities of different sequences change, depth (km) is approximately 1.5 × two-way time (s).

vertical fluid drives, they do not, on their own, highlight the nature of basinal flow.

Faults as barriers to basinal flow

The importance of fault sealing within basins has long been recognized (e.g., Allan, 1989; Knipe, 1992; Lindsay et al., 1993), principally because many hydrocarbon reservoirs are fault traps, with faults representing either juxtaposition seals, by juxtaposing impermeable units against reservoirs, or membrane seals, in which low-permeability fault rocks support hydrocarbon columns because of their high capillary entry pressures (Gibson, 1994; Yielding et al., 1997; Manzocchi et al., 2010). In mixed clastic sequences, faults act as barriers to flow within reservoir/aquifer sandstones mainly because associated fault rocks are derived from the cataclasis and clay smearing of interbedded host rocks with significant clay content (Fig. 5a). Whereas fault sealing within carbonate sequences is less well understood, clay-rich host rocks are also likely to provide a basis for forming clay smears and dissolution-related clay restites. In this paper, we restrict our consideration of fault sealing to siliciclastic sequences, concentrating on the sealing of aqueous fluids rather than the generation of hydrocarbon traps, an issue that is referred to in a later section.

Pressure compartmentalization of basins: In basins where there is sufficient drilling coverage, it is possible to investigate the spatial variation of pore fluid pressures. Regional-scale maps of the North Sea show that high overpressures (>20 MPa) are developed within the main basin grabens, such as the North Viking graben, with pore-fluid pressures that are strongly compartmentalized by faults (Fig. 2; Nordgård Bolås and Hermanrud, 2003). Even on a smaller scale, the role of fault compartmentalization is clear, with individual aquifers, such as the relatively clean Late Jurassic Tarbert sandstones (Fig. 2), developing distinct pressure compartments even

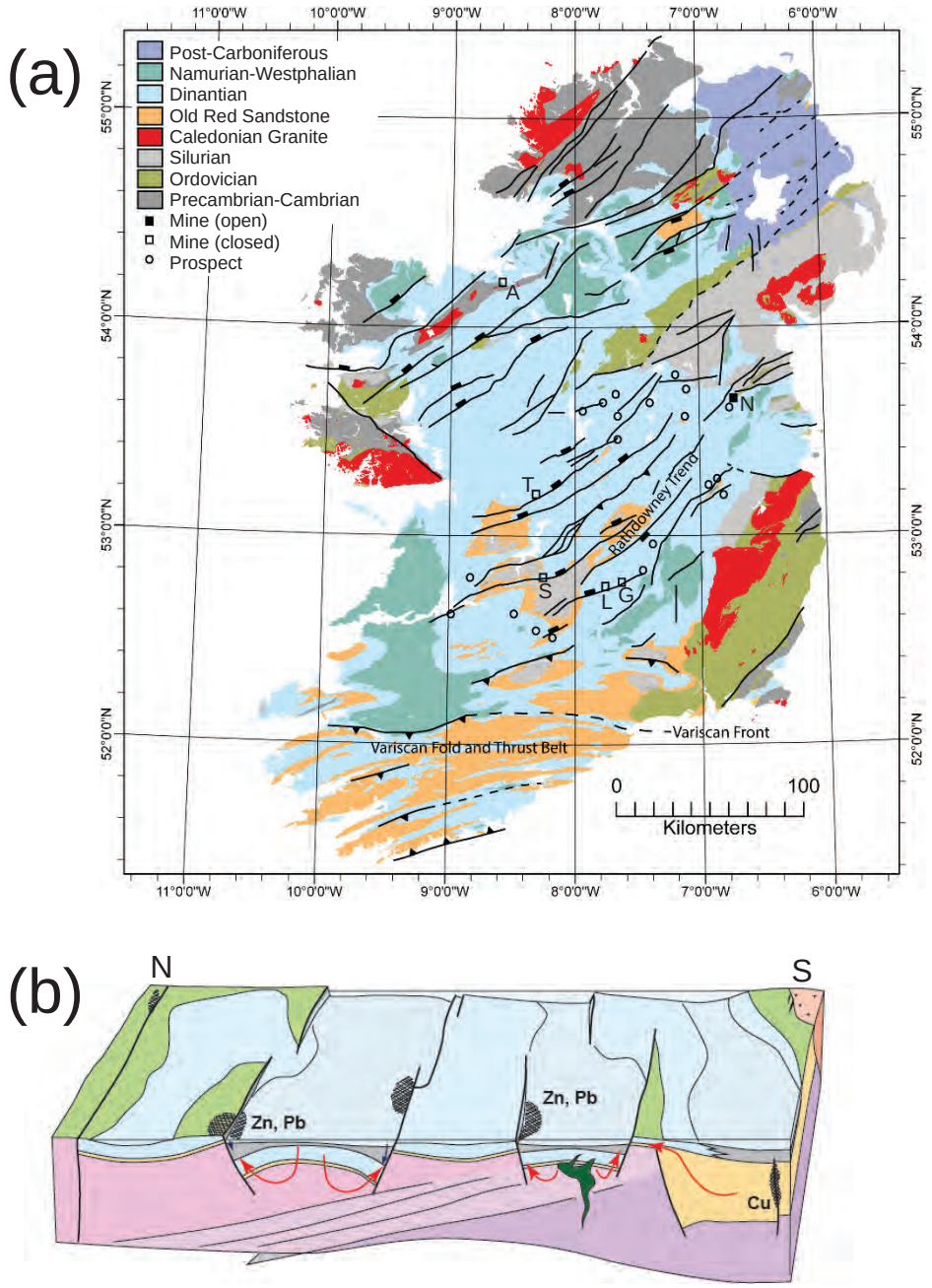

Fig. 3. (a) Geologic map of Ireland showing the main stratigraphic units and the locations of the main Irish-type Zn-Pb deposits, including the active mine (black-filled square; N = Navan), closed mines (open squares; A = Abbeytown, G = Galmoy, L = Lisheen, S = Silvermines, T = Tynagh), and prospects (open circles). The main host rocks of the deposits are the early Carboniferous (i.e., Dinantian) limestones (light blue). (b) Schematic diagram showing Carboniferous extensional basins, with discontinuous faults, mini basins, convection cells, volcanic rocks/granite, and Zn-Pb and Cu mineral deposits. Limestones are shallow-water (blue) and deep-water (blue-gray) basin facies, and sometimes become emergent (light green) in the footwalls of major faults. Underlying lower Paleozoic and older basement rocks in the south (purple) and north (pink) are separated by a shallow-dipping zone of terranes accreted along a northward-dipping subduction zone prior to the Caledonian orogeny. The Munster Basin in the south is a major Upper Devonian depocenter infilled by Old Red Sandstone (yellow), which thins dramatically northward but nevertheless extends to the north of Ireland. The lower Carboniferous Limerick volcanic rocks (deep green) and the margin of the Caledonian Leinster granite (red) are shown. Red arrows are deep convection flow paths, and blue arrows are along-fault paths for sinking dense brines.

across faults that have displacements less than the aquifer thickness. This feature demonstrates that faults are acting as low-permeability barriers to across-fault fluid flow. Three-dimensional modeling of the Tune area on the eastern flank of the North Viking graben has shown that pressure compartmentalization arises from fault sealing, with significant pressure changes (12 MPa) maintained across a small displacement (approximately 50 m) fault offsetting the 100-m-thick Tarbert

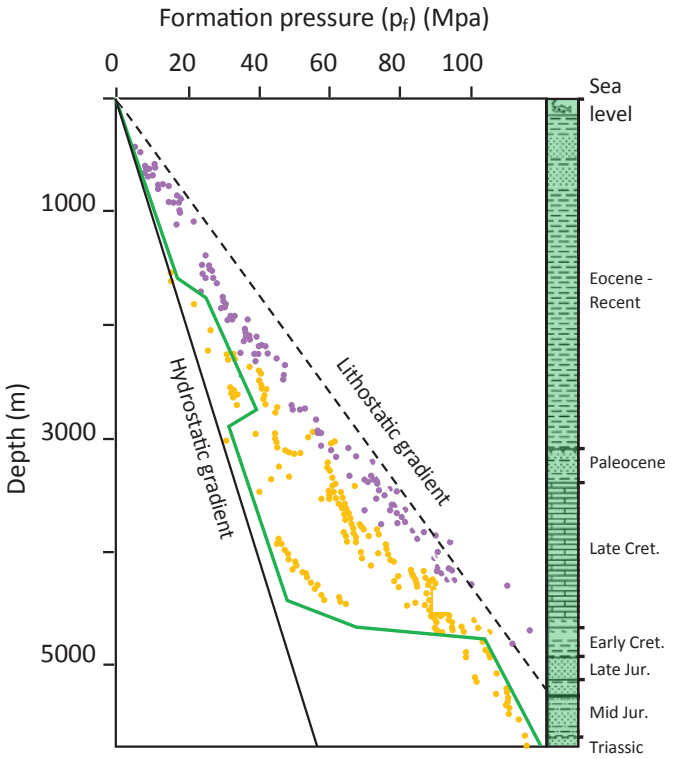

Fig. 4. Pore fluid pressures (yellow) and leak-off pressures (purple) as functions of depth for multiple wells from the North Sea Central graben (from Gaarenstroem et al., 1993; Nordgård Bolås and Hermanrud, 2003). The pore fluid pressure ratio, λ, is the ratio between the fluid pressure and the rock (i.e., lithostatic) pressure. Pore fluid pressures range between the hydrostatic gradient, where pore fluids are open to the surface and $\lambda = 0.4$, and the lithostatic gradient, where the interstitial pore fluids entirely support the rock column and $\lambda = 1.0$. The pore fluid pressure curve and corresponding stratigraphic column (both in green) for a single well from the Central graben (Holm, 1998) highlight the variability of pore fluid pressures with depth along individual wells, which arises from 3D changes in lithology and connectivity of permeable and impermeable units. Leak-off pressure is the pressure at which a fluid within the wellbore begins to leak off into the surrounding rock, either by moving through permeable paths or by fracturing the rock. Sometimes referred to as the fracture pressure, it is often taken to be the minimum fluid pressure at which fractures are created and generally occurs at fracture gradients of $\lambda > 0.8$.

sandstone aquifer, which contains a single approximately 10 m thick clay interbed (Fig. 6; Childs et al., 2002). Despite the variable displacements on individual faults and the associated spatial variations in across-fault sequence juxtapositions, compartmentalization can be very pronounced, suggesting a combined role for both juxtaposition and fault sealing. Relatively complex flow pathways are indicated by the fact that, whereas the compartmentalization of different aquifers is generally similar, they need not be the same, with some compartments depressurized relative to adjacent blocks (Fig. 2c).

Fault seals and their hydraulic properties: The impact of faults on the compartmentalization of basinal fluids is dependent on the thickness and permeability of associated fault rocks. Estimates of fault rock thickness can be derived from empirical constraints defining the approximately linear increase in fault rock thickness with displacement (Fig. 5d; Walsh et al., 1998; Manzocchi et al., 1999). Even though individual fault surfaces are characterized by small-scale spatial variations in fault rock thickness (Childs et al., 2009a), previous studies have shown that existing empirical data can be used to model across-fault fluid flow (e.g., Childs et al., 2002; Jolley et al., 2007b; Manzocchi et al., 2008b). Fault rock permeabilities are constrained by laboratory measurements of different types of fault rock, with the most important controlling factor being the clay content (Manzocchi et al., 1999; Fisher and Knipe, 2001). Existing hydrocarbon industry algorithms for fault permeability prediction within mixed clastic sequences assume that the clay content of fault rocks is in some way related to the clay content of the sequence that has moved past a point on a fault. The most commonly used algorithm, the shale gouge ratio (SGR; Yielding et al., 1997, 2010), assumes a direct equivalence between % clay in the faulted sequence and associated fault rock, a relatively rudimentary approximation that has nevertheless provided a much-improved basis for reservoir modeling and production forecasting (Jolley et al., 2007b). Predictive algorithms are underpinned by fault permeability data for different types of fault rock (Fig. 7; Fisher and Knipe, 2001; Yielding et al., 2010), the origins of which are discussed below.

Many factors control the nature and permeability of fault rocks within mixed clastic sequences, but the clay content and depth of burial at the time of faulting are believed to be the most important (Fisher and Knipe, 2001; Yielding et al., 2010; Kristensen et al., 2013). At shallow burial depths (<~500 m) and lower confining pressures, fault rock generation involves grain flow and smearing, forming disaggregation zones or bands in sandstones and clay smears within muddier facies sequences. Disaggregation does not significantly affect permeability, but the impact of clay smearing on the effective properties of a fault are profound. Outcrop studies have shown that where low-permeability clays are smeared along a fault, they commonly show significant lateral (i.e., spatial) persistence, in a manner similar to deformed layers within ductile shear zones, and irrespective of fault displacement (Lehner and Pilaar, 1997; Bence and Person, 2006; van der Zee and Urai, 2006). In these circumstances, faults affecting a mixed sequence of layers have effective cross-fault permeabilities that are governed by the harmonic average of the layer permeabilities (as opposed to the arithmetic mean; Pickup et al., 1995; Walsh et al., 1998), such that

$$k_h = \left[\frac{\sum_{i=1}^{n} t_i/k_i}{\sum_{i=1}^{n} t_i} \right]^{-1}, \quad (3)$$

where i is the number of the layer, n is the total number of layers, and k_i and t_i are the permeability and thickness, respectively, of the number i layer. This expression means that across-fault rock properties are dominated by those of the very low permeability clays in a clastic sequence (Walsh et al., 1998). This is highlighted by the strongly nonlinear curve (Fig. 7b), derived from equation 3, defining the associated across-fault permeability of faults contained within mixed clastic sequences of interbedded high-permeability sandstones (10,000 mD) and low-permeability clays (0.0001 mD),

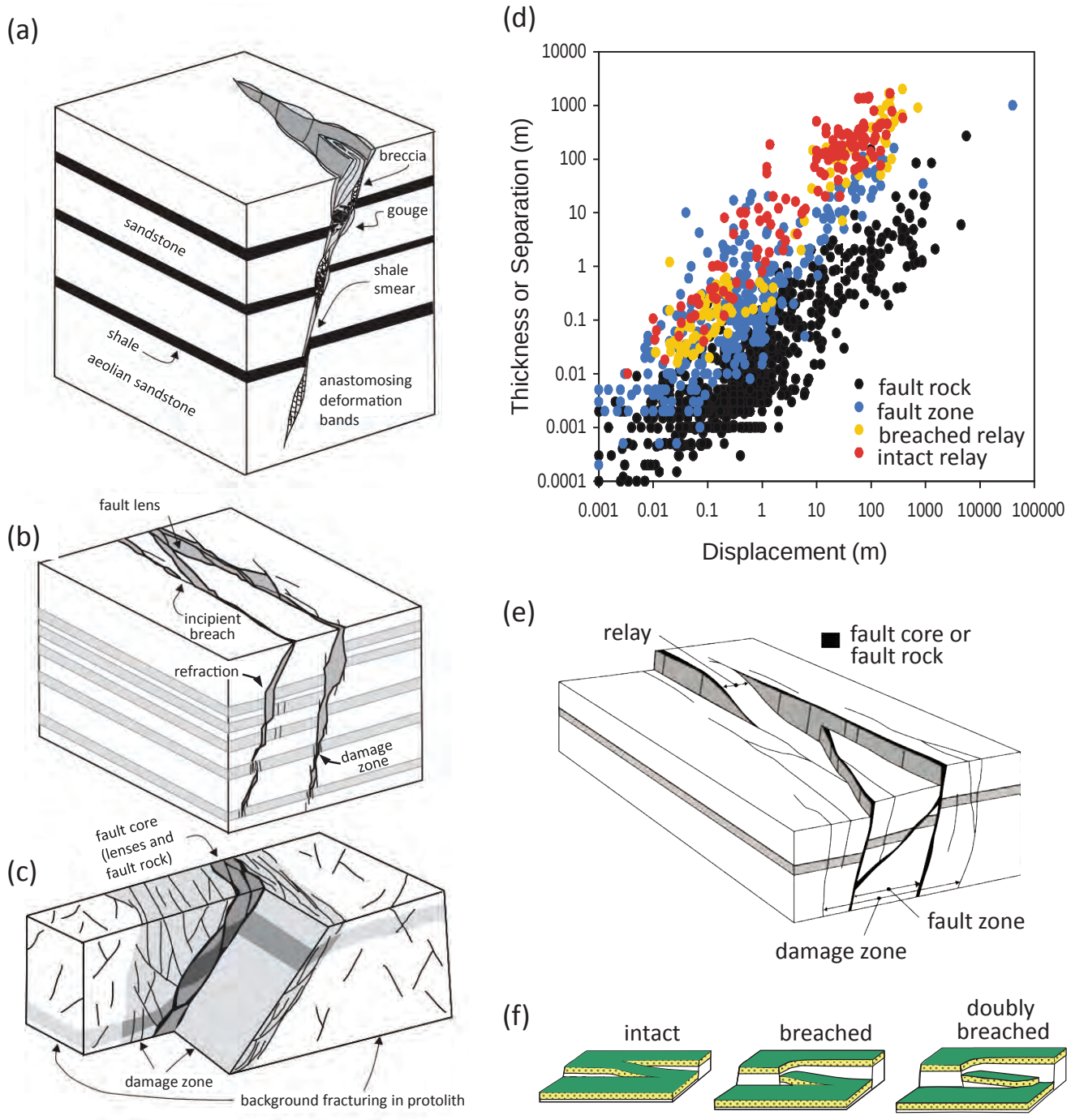

Fig. 5. Schematic diagrams comparing a selection of conceptual models of fault zones. (a-c) All cartoons in the left-hand column have a normal sense of offset with the downthrown side on the left and with (b) also having a dextral strike-slip component of displacement (Manzocchi et al., 2010). (a) A fault in a sand-shale sequence (after Walsh et al., 1998). The fault zone comprises lensoid volumes of fault rock bounded by discrete slip surfaces. Fault rock is derived from adjacent host rock, with breccia (>30% visible fragments), gouge (<30% visible fragments), and shale smears. In poorly lithified sediments in the top few kilometers of basins, breccias are less often developed and shale smears can be very continuous and shear zone-like. (b) A fault in a strong/weak sequence (after Wibberley et al., 2008) in which faults have high dips within strong layers (sandstones/limestones) and lower dips within weaker layers (shales/clays). (c) A fault annotated according to the fault core/damage zone conceptualization of Caine et al. (1996) (after Berg, 2004). (d) Thickness (or separation) versus displacement plot for the four fault geometric components used in defining the fault zone model of Childs et al. (2009a). (e) Schematic diagram comparing the terms fault rock, fault zone, and relay zone used in the Childs et al. (2009a) model, with the fault core/damage zone description. Fault rock is synonymous with fault core sensu Caine et al. (1996). At the center of the block diagram (along the dashed line), the bulk of the displacement is accommodated on a single slip surface and, therefore, the fault zone thickness is equal to the thickness of the fault rock/fault core. Thin lines indicate faults with minor displacements. (f) Schematic diagrams of intact relay, breached relay, and doubly breached relay.

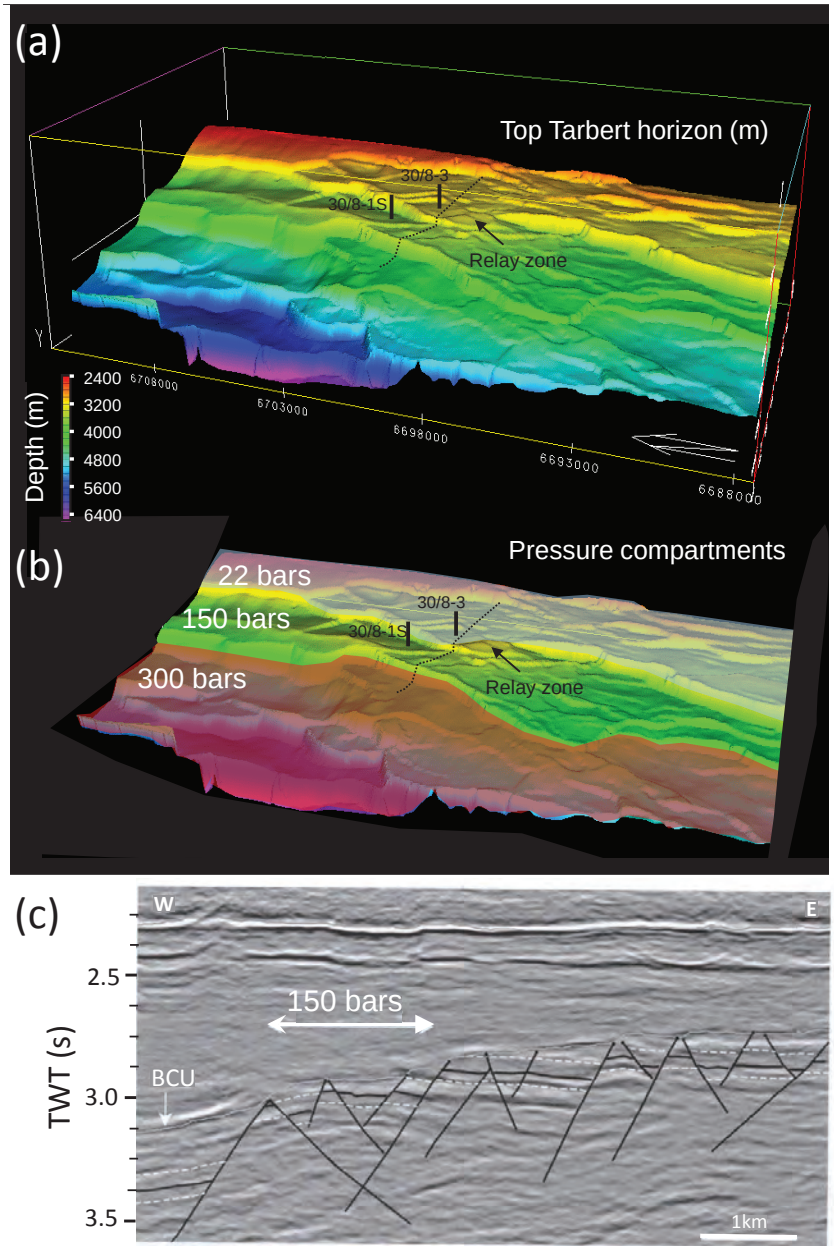

Fig. 6. Late Jurassic (Top Tarbert) depth (a) and overpressure (b) model for 25-km-long area from the Tune field, North Viking graben; see red box in Figure 2b for location. Depths are in meters, and faults are marked by rapid depth drops extending along strike. North arrow is in bottom right-hand side of the model and is along the length of the area. A relay zone between two major faults is highlighted, but there is still a 120-bar (12 MPa) pressure drop between the two wells shown. Faults provide pressure compartmentalization for this 150-m-thick unit even when the fault displacements are of ~50 m, less than the reservoir thickness: a critical determinant of related fault properties is the presence of an 8-m-thick shale unit in an upper 100-m-thick sandstone of the Tarbert sequence (see Childs et al., 2002, for further details) and a mainly clay rich (~40%) sequence in the bottom 50 m. (c) Seismic section across the Tune area (location shown in a) with interpretation of the Top and Base Tarbert reservoir (broken lines) and the top of the clay-rich bottom part of the sequence (solid line). Depth is in seconds two-way travel time (TWT) and, while the velocities of different sequences change, depth (km) is approximately 1.5 × two-way travel time (s). BCU = Base Cretaceous Unconformity.

over the full range of % clay interbeds. For depths greater than about 500 m at the time of faulting, cataclasis (i.e., fracturing and comminution) and the mixing of host rocks become the dominating fault rock deformation processes (Fisher and Knipe, 2001; Kristensen et al., 2013). This leads to the formation of deformation bands within sandstones through to more clay-rich fault rocks, such as phyllosilicate framework fault rocks, in which clays generate a connected framework, and shale gouges, which are dominated by clays (see Fig. 7; Fisher and Knipe, 2001; Yielding et al., 2010). These cataclastic fault rocks are also characterized by a strongly nonlinear relationship between permeability and clay content (Fig. 7b).

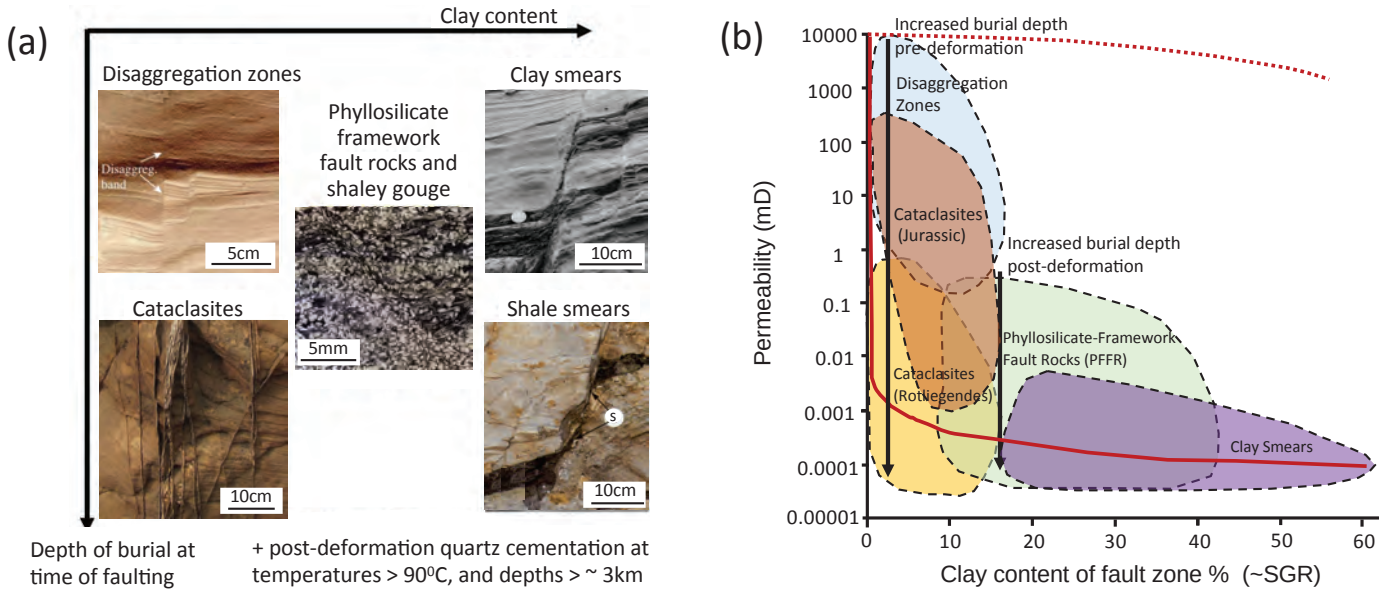

Fig. 7. (a) Schematic diagram of the main fault rock types generated within siliciclastic (sand-clay) sequences in sedimentary basins (modified from Yielding et al., 2010). The axes represent two of the three main controls on fault rock permeability: clay content and depth of burial at the time of faulting (which is a proxy for stress conditions). The third main control is postfaulting temperature history, which is mainly reflected in quartz cementation at temperatures above 90°C and depths in excess of 3 km. Photographs are from Lindsay et al. (1993), Fristad et al. (1997), van der Zee and Urai (2005), Fossen et al. (2007), and Nicol et al. (2013). Arrows highlight the location of disaggregation bands and shale smears on their respective photos. (b) Summary of fault rock permeability data from the North Sea and Norwegian continental shelf. Permeability is plotted against clay content for the various fault rock types. Also shown are two of the main controls on the permeability of the faults in clean sandstones and impure sandstones: burial depth at the time of faulting and maximum postdeformation burial depth, respectively (black arrows). Two red curves are shown for the effective permeability for across-fault flow (solid line) and along-fault flow (broken line) of a shear zone fault model comprising 10,000-mD sandstones interbedded with 0.0001-mD clays, with clay % representing the proportion of clays within the sequence (equivalent to the shale gouge ratio, SGR, of the fault zone; see text for details).

The foregoing discussion shows that clay-rich cataclastic fault rocks and ductile clay smears have permeabilities that are up to several orders of magnitude lower than interbedded sandstone aquifers/reservoirs. Recent hydrocarbon-related case studies demonstrate that these processes and associated fault rocks are capable of generating fault-bounded pressure compartments on a broad range of scales, from regional to reservoir (Childs et al., 2002; Jolley et al., 2007a, b; Manzocchi et al., 2010). Because normal faults act as barriers to out-of-basin lateral flow, associated overpressuring can eventually provide conditions favoring up-fault flow. In that sense, fault-controlled pressure compartmentalization provides the basic hydrodynamic backdrop not only for basinal flow, but also for potential upward fluid flow along faults, an issue considered in the next section, and a prerequisite for the generation of mineral deposits and hydrocarbon reservoirs.

Fluid pressure-driven up-fault flow

Here we consider up-fault flow in circumstances where overpressure-driven fluid migration involves either static or dynamic interaction with normal faults, in which faults act either as passive pathways or valves for up-fault fluid flow (Sibson, 2000, 2001; Bence and Person, 2006). Because normal faults can provide juxtaposition or membrane barriers to lateral flow, it may at first appear contradictory to suggest that the same faults can act as pathways for up-fault flow (Bence and Person, 2006; Childs et al., 2009b). Consideration of the effective permeabilities of faults indicates, however, that they can display a duality of flow behavior by preventing cross-fault flow and permitting up-fault flow.

Faults as passive pathways for flow: Whether fault rocks comprise clay smears or cataclastic mixtures of clays and mudstones, the decrease in fault rock permeability with clay content is nonlinear (Fig. 7). The effective properties of clay smears for across-fault flow range from the lower bounds of the fault permeability-clay content distribution (Fig. 7), reflecting a shear zone geometry in which multiple clay smears arise from shear of the entire sequence into the fault, to the upper bounds of the permeability distribution, in which the clay smears are more discontinuous and cataclastic fault rocks are an admixture of comminuted clays (i.e., phyllosilicates) and other lithic grains (Childs et al., 2007). Ultimately, the end-member curves presented in Figure 7 highlight the importance of the internal structure of fault zones to their impact on flow.

The significance of fault zone structure can be explored further by considering the flow anisotropy of a simple shear zone model in which a sequence is attenuated along the fault zone. As we have seen, the effective properties for cross-fault flow of a shear zone model are the harmonic average of all of the layers, which in this case is equivalent to the vertical permeability of the host-rock sequence (K_v). Such a fault will, therefore, represent a barrier to cross-fault flow, in the same way that sand-clay sequences act as barriers to vertical flow. The effective properties for along-fault flow within a shear

zone-type model are, however, the arithmetic average of all of the layers, such that

$$k_a = \frac{\sum_{i=1}^{n} k_i/t_i}{\sum_{i=1}^{n} t_i}, \quad (4)$$

an expression representing a much higher effective permeability than the K_v of the faulted sequence.

The above flow considerations show that faults that are barriers to cross-fault flow can also be pathways for up-fault flow, an attribute reflecting their conduit-barrier behavior (Bence and Person, 2006). Of course, normal faults do not commonly conform to a simple shear zone model, but the internal anisotropy within faults, in which mineral and structural alignments are developed parallel to the fault zone, will provide flow anisotropies that facilitate up-fault flow rather than across-fault flow. As a consequence, faults may be sealing to cross-fault flow within aquifers, but they still represent the most effective means of passive upward flow. Given the heterogeneous nature of faults (Childs et al., 2009a), up-fault flow is, however, likely to be very heterogeneous, an issue we return to later.

Fault valving: A more conventional mechanism for up-fault flow involves the valve-like behavior of overpressured fluids along or adjacent to faults (Phillips, 1972; Sibson, 1992, 2000). We consider fault valving here because it is an important means of fault-related fluid flow in postrift basinal sequences, even though it is commonly applied in circumstances where faults are tectonically active. This model is also implicated in the formation of vein-hosted mineral deposits, typically within competent low-porosity and low-permeability basement rocks (volcanic, plutonic, metamorphic), either in orogenic belts (see Sibson, 1990; Boullier and Robert, 1992; Cox et al., 1995) or underlying sedimentary basins (Sibson, 2000). Because this mechanism does not require contemporaneous tectonic activity and associated earthquake (i.e., coseismic) slip events, we use the term fault valving rather than seismic valving. In seismically active regimes, fault valving nevertheless provides a means of triggering earthquakes and can be inextricably linked to the earthquake cycle. Here we outline the basic principles of fault valving and will briefly consider its implications for earthquakes in the next section.

Fault valving involves the buildup of overpressures within and below impermeable units, leading to fault failure and up-fault fluid flow. Valve behavior is schematically illustrated by a normal fault transecting a stratigraphic seal capping either uniformly overpressured crust or overpressures localized within or adjacent to a fault zone at depth (Fig. 8; Sibson, 2000). The associated readjustment and decrease in overpressure are subsequently followed by pressure buildup arising from further burial and basinal flow, perhaps accompanied by an increase in regional stress, until another valving event occurs. In that sense, basin overpressure profiles and fault valving are coupled as the preexisting or new faults or fractures buffer the overpressure buildup (Sibson, 2000). A reflection of the coupling of overpressure and fracture-related valving is seen in basins like the North Sea, where tests of hydraulic failure indicate the presence of a fracture gradient at λ values of approximately 0.8,

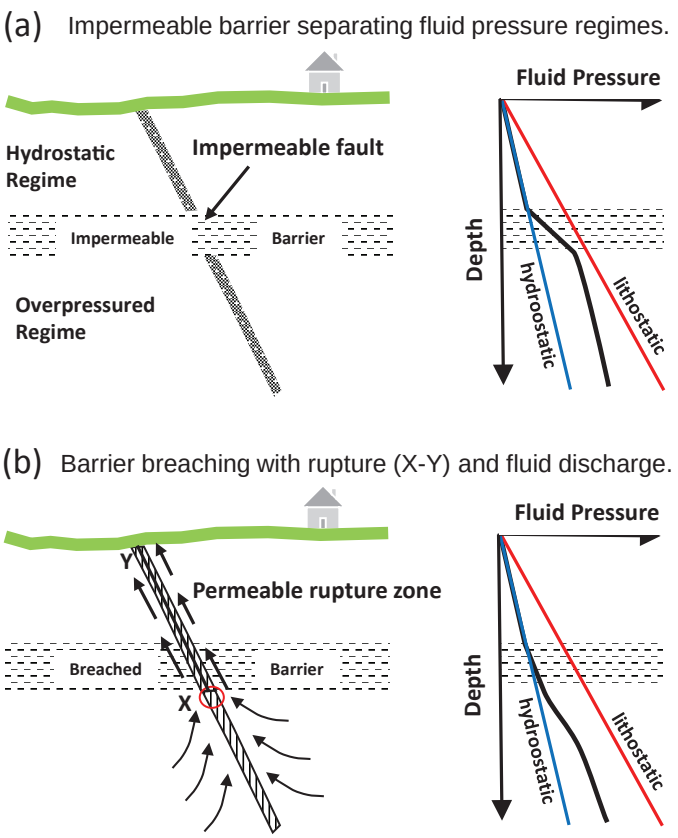

Fig. 8. Potential for fault-valve behavior, illustrated by schematic diagrams and pore fluid pressure profiles. (a) Impermeable barrier separating hydrostatic and overpressured fluid pressure regimes. (b) Breaching of barrier by fault rupture X-Y, leading to an upward discharge of fluids. Modified from Sibson (1990).

at or above which faults/fractures valve (Fig. 4). This valving can arise from the generation of new hydraulic fractures or the reactivation of existing faults (Sibson, 2000). Which of these occurs depends principally on the differential stress, the stress difference between the maximum principal stress, which in an extensional basin is vertical (σ_v), and the minimum horizontal stress (σ_h), which is typically perpendicular to the prevailing normal fault orientation in an active rift (Fig. 9).

Models exploring the conditions for fracture-controlled valving of fluids investigate the stress/fluid-pressure conditions for different modes of failure using a Mohr diagram of shear stress, τ, vs. normal stress, σ_n, with a composite Griffith-Coulomb failure envelope for intact homogeneous rock and a straight failure envelope for a cohesionless preexisting fault (Fig. 9). Here we concentrate on the main features of these models, but readers are referred to Sibson (2000) and Cox (2005) for further details. Stresses are conveniently referred to in terms of multiples of the tensile strength (T) because it can be linked directly to the shape of the failure envelope, which intersects the normal stress axis at –1T and the shear stress axis at 2T (Fig. 9; Secor, 1965; Sibson, 2000). In an active rift, σ_1 is the lithostatic load, and σ_3 combines the (negative) horizontal regional stress and the elastic response to the vertical load. In the absence of tectonic stresses,

$$\sigma_3 = (\nu/(1-\nu)) \cdot \sigma_1, \quad (5)$$

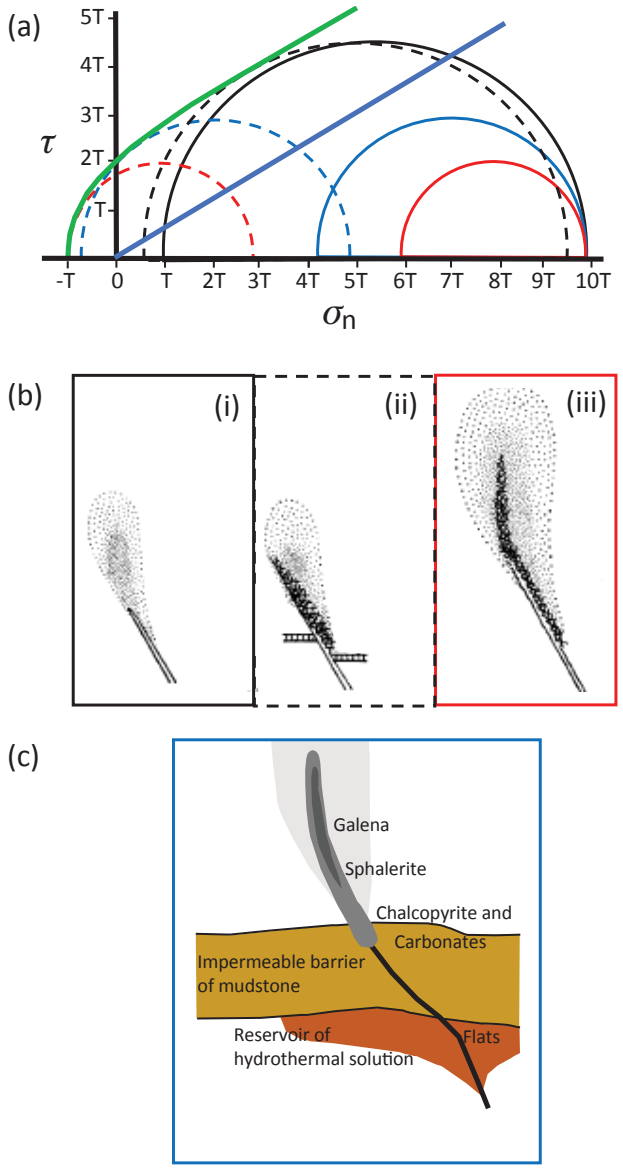

Fig. 9. (a) Models investigating the stress/fluid pressure conditions for different modes of failure using a Mohr diagram of shear stress, τ, vs. normal stress, σ_n, with a composite Griffith-Coulomb failure envelope (green) for intact homogeneous rock normalized to tensile strength, T (after Secor, 1965), and a straight failure envelope (blue) for a cohesionless preexisting fault. See text for details. (b) Schematic diagrams showing the structures developed during particular stress conditions (from Phillips, 1972)—the boxes surrounding (i), (ii), and (iii) correspond to Mohr circles with the same line type in (a). The first is a zone of dissemination/permeation from a fault that has not failed. The second is a zone of hydraulic fracturing and brecciation (dark color) associated with a fault that shows failure in shear. The third is vertical hydraulic fracturing at low differential stress (<4T). (c) The effect of an impermeable mudstone unit on the development of mineralization associated with Zn-Pb Wales orefield vein systems (Phillips, 1972).

where ν is Poisson's ratio. The application of a horizontal tensile stress decreases σ_3 and increases the stress difference (i.e., the differential stress between σ_1 and σ_3) of the Mohr circle representing the prevailing stress conditions. Whatever the stress difference, the effect of overpressure is to decrease all principal stresses by the pore fluid pressure (P) to provide the effective normal stresses of the system (Terzaghi's law). Overpressures therefore move stress circles to the left, so that they intersect the failure envelope.

The type of fracture that is generated depends on the differential stress of the associated Mohr circle. An intercept along the straight portion of the failure envelope requires higher differential stresses (>5.66T) and leads to shear failure along faults (i.e., shear fractures) with dips of 60° to 70°, whereas for lower differential stresses (<4T) the smaller Mohr circle will only intersect the failure envelope at –1T, generating vertical extension fractures (i.e., veins): differential stresses of 4T to 5.66T will provide hybrid, shear-extension fractures. For a rock containing a cohesionless fault which is suitably oriented, failure will always involve fault reactivation, rather than the generation of newly formed vein networks (Sibson, 2000). The latter conditions will apply to faults formed during the formation of an extensional basin, whether those faults are tectonically active or not at the time of valving.

The importance of fault valving in the formation of mineral deposits was first advocated by Phillips (1972) in his study of the Zn-Pb vein deposits in central Wales. His model considers the role of differential stresses, with high differential stresses providing hydrothermal plumes without failure (Fig. 9bi) through to shear failure and fault mineralization (Fig. 9bii), and with low differential stresses providing arrays of steep hydrothermal veins extending above fault tips (Fig. 9biii). Whatever the circumstances, mechanical failure will lead to the valving of overpressured fluids, with the subsequent buildup of overpressures leading to another valving event. Given the progressive loading of sediments within deepening basins, even after rifting has ceased, overpressuring will be punctuated by multiple valve events, providing a means of fluid migration. The repercussions of this mechanism for mineralization will be discussed later, but first we outline other flow-related phenomena, in the context of faults that are seismically active.

Fluid flow driven by active faulting

The perception of many geologists is that, for faults to have an impact on fluid flow, they must be seismically active. The foregoing discussion shows that up-fault valve-like behavior and fault sealing can occur long after fault activity and related rifting have ceased. Faults within the North Sea, for example, have been tectonically inactive for the past 145 m.y., but they still exercise a major control on subsurface fluid flow. Nevertheless, the participation of active faults within flow systems does provide a variety of mechanisms for driving fluid flow. Three principal dynamic mechanisms, linked to the seismic stress cycle, contribute to fluid redistribution associated with normal fault systems (Sibson, 2000). The first, fault valving, provides a means of transporting fluids during coseismic events, with overpressures triggering or facilitating earthquake events. The second mechanism is seismic pumping, which is related to the cycling of mean stress coupled to shear stress and provides for the large-scale redistribution of fluids within the volume surrounding a fault over a seismic cycle (Sibson et al., 1975; Muir-Wood and King, 1993), particularly immediately following an earthquake. The final mechanism is seismic pulsing, which involves a suction pump action associated with fault dilatancy during a coseismic event (Wilkins and Naruk, 2007). Here we describe the main principles of seismic pumping and seismic pulsing.

Seismic pumping: This model, first developed by Muir-Wood and King (1993), integrates the volumetric changes associated with a seismic cycle on a normal fault by considering the dilations linked to the buildup of elastic strain during interseismic periods through to the mainly compressional strains associated with coseismic movement. Their model was developed in response to and informed by hydrological data for coseismic groundwater flow associated with normal faults within the Basin and Range province, USA, and the Pennines, Italy. The backdrop to this model is that faults and earthquakes induce strain within the host rock, which varies along a fault from maximum to minimum displacement (Fig. 10). For normal faults, this deformation takes the form of footwall uplift and hanging-wall subsidence, which occur both on short timescales associated with earthquake events and on long timescales reflecting isostatic deformations (Fig. 10a). This is illustrated for the Lost River fault in the Basin and Range province, a normal fault with vertical displacement of over 4 km (Fig. 10c; Stein and Barrientos, 1985). The long-term balance between uplift and subsidence across this fault is isostatically controlled (King et al., 1988) and partly arises from erosion and unloading of the footwall and by limited sediment deposition within the hanging wall of the fault.

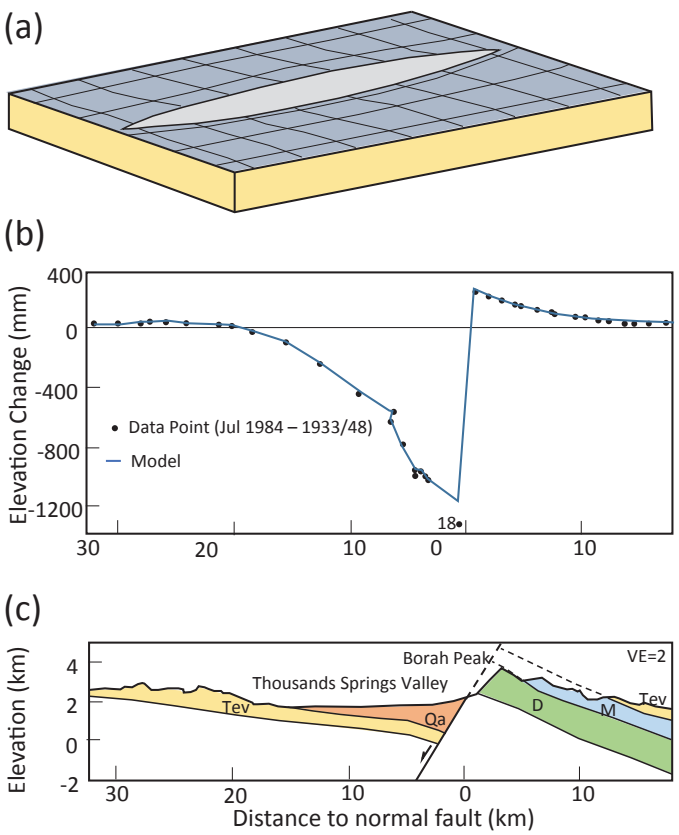

Fig. 10. (a) Deformation surrounding a single normal fault, showing footwall uplift and hanging-wall rollover. (b) Profile of observed coseismic elevation change for the Borah Peak 1983 earthquake (dots), together with predicted changes (line) for the coseismic model: kinks in the model profile result from changes in azimuth of the leveling route. (c) Schematic cross section of the Lost River fault showing Devonian (D) and Mississippian (M) limestones, Tertiary volcanic rocks (Tev), and quaternary alluvium (Qa). From Stein and Barrientos (1985). Vertical exaggeration (VE) is ×2.

Together, these have accentuated the footwall uplift, providing a significant hydraulic head from footwall into hanging wall and leading to conditions that are important from a fluid circulation perspective. The shorter-term coseismic strains that accompany individual earthquakes, however, have other, very different implications.

Between seismic events, within the interseismic phase, the long-term deformation of the volume surrounding a fault is the result of a slowly accumulating extensional stress that is accommodated by elastic dilations of the host-rock volume, either through fracturing or poroelastic effects (Sibson et al., 1975; Muir-Wood and King, 1993). This will have the effect of increasing host-rock permeability between events. Where the stresses exceed the shear stresses on the fault, an earthquake will occur, with associated instantaneous slip accommodated by footwall uplift, hanging-wall subsidence, and the imposition of compressional strains that can be modeled by elastic dislocation theory (Fig. 10b). These strains can be modeled in 3D and provide a means of predicting the spatial variations in volume loss accompanying an earthquake (Fig. 11).

Muir-Wood and King (1993) showed that coseismic porosity losses are consistent with accentuated surface flow measured within the deformation volume of two major earthquakes in the Basin and Range province: the Borah Peak 1983 earthquake (M6.9) on the Lost River fault and the Hebgen Lake 1959 earthquake (M7.3) on the Hebgen Lake and Red Canyon faults (Fig. 11a). The associated volumetric changes are considerable, with 0.3 and 0.5 km^3 of water expelled during the Borah Peak and Hebgen Lake earthquakes, respectively—earthquakes marked by maximum displacements of 4 and 6 m. Assuming 1,000 such earthquakes to form the km-scale displacement faults we see would provide fluid volumes of 3×10^2 km^3 and 5×10^2 km^3. This number of earthquakes is consistent with plausible, ca. 20,000-year repeat times and 17-m.y. Basin and Range rifting (Wallace, 1987; Mouslopoulou et al., 2009). These magnitudes of earthquake-driven flow are only observed within normal fault systems because strike-slip earthquakes are characterized by much lower volumes of coseismic flow (~10%), with reverse earthquakes showing little if any flow (Muir-Wood and King, 1993). The substantial volumes of fluids concerned mean that, within extensional sedimentary basins, seismic pumping associated with normal faults can be a major driver for fluid flow (Blundell, 2002).

Seismic pulsing: The second form of fault-driven fluid flow is referred to as seismic pulsing, in which earthquake slip and frictional sliding cause transient dilation (i.e., opening) and the pulsing of fluids up the fault surface (Wilkins and Naruk, 2007). Seismic pulsing differs from seismic pumping insofar as it considers the amount of flow that can be localized along an individual fault during an earthquake event, rather than the larger volumetric strains associated with an earthquake event (Fig. 12a). Faults that accumulate displacement by aseismic slip (i.e., without earthquakes) will not show the same dilations and will, instead, have up-fault flow properties equivalent to the static along-fault permeabilities considered in the previous section. The seismic pulsing model was informed by geophysical data indicating the importance of propagating slip pulses characterized by transient dilation during earthquake slip events and by quantitative laboratory constraints on the porosity evolution during frictional sliding.

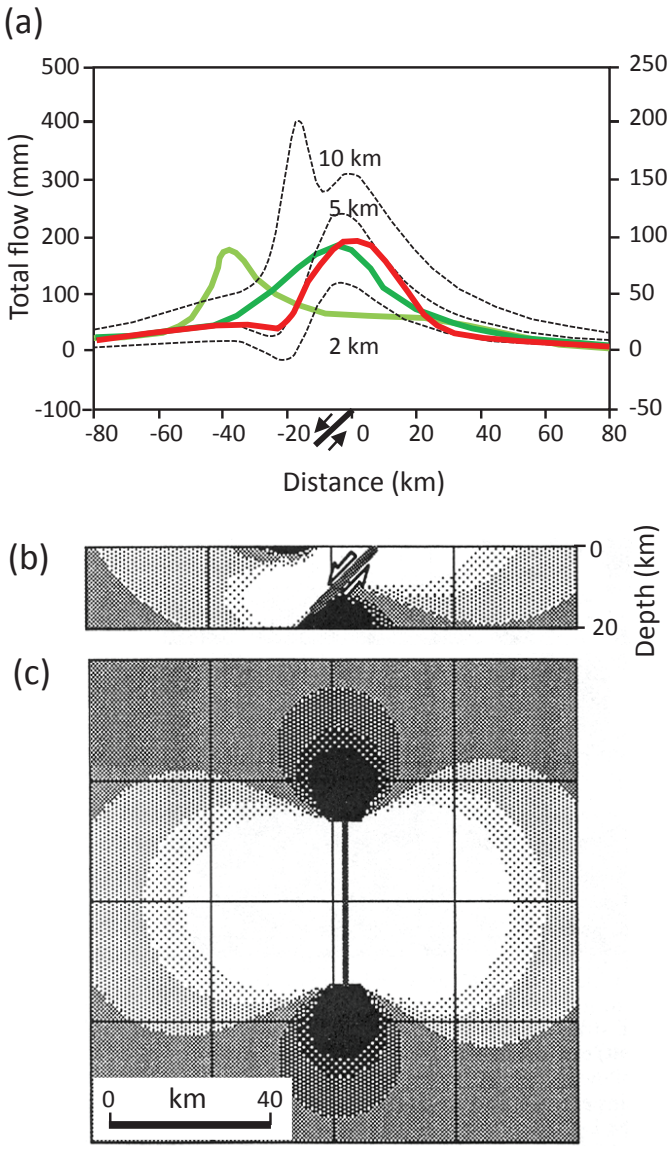

Fig. 11. (a) Observed and predicted total flow for cross sections perpendicular to the Hebgen Lake (red) and Borah Peak earthquakes (green curves), in which cumulative rainfall-equivalent discharges along a traverse perpendicular to the strike of each of the faults are compared with those predicted for a two-dimensional strain model (Muir-Wood and King, 1993): the light green curve is across the Upper Lost River tributaries, whereas the dark green curve is interpolated around the fault where there was significant water loss in the broad Lost River Valley. The scales for Hebgen Lake and Borah Peak are on the left- and right-hand side of the plot, respectively, with predictions derived from fault models for a constant slip of 6 and 3 m, and a fault dip of 45° extending to a depth of 1 km. The predicted curves are based on the assumption that the areal strain summed to depth ranges of 2, 5, and 10 km (dotted lines) is expressed as a change of porosity and a corresponding appearance of displaced water (in mm) at the surface. (b) Cross section and (c) plan view of strains modeled at a depth of 5 km around a 45°-dipping normal fault in a half-space. Strain levels are shaded from a background gray to lighter shades (negative strain, i.e., compressional strain) and to darker shades (positive strain) in strain steps of 2×10^{-5}. Modified from Muir-Wood and King (1993).

Seismic pulsing involves a process in which a slip pulse void, defined by a dilatancy-driven pressure drop, instantaneously forms and then propagates along the margin of a fault (Fig. 12a). Host-rock fluids fill this void to equilibrate the pressure decline and travel up the fault for some undeterminable distance (for further details, see Wilkins and Naruk, 2007); this process is similar to the seismic suction pump effect described by others (Rudnicki and Chen, 1988; Grueschow et al., 2003). The fluid volumes mobilized in a slip event are linked to the amount of slip and associated dilation, which are in turn controlled by the size of the earthquake and, therefore, the fault length (on the basis that fault length correlates with earthquake slip; Wells and Coppersmith, 1994). The repeat time of associated earthquakes will dictate fault displacement rates and the cumulative amount of fluid expelled. Other factors include the rupture velocity and earthquake rise time—parameters that are discussed by Wilkins and Naruk (2007). Figure 12b shows the volume of leaked fluids for faults with different lengths and for representative displacement rates: fault displacement rates vary with fault length and from basin to basin (Mouslopoulou et al., 2009), depending on regional strain rate, but consideration of this variability is beyond the scope of this paper. Associated curves suggest that, for representative displacement rates of between 0.1 and 1 mm/year, a 30-km-long fault can provide up-fault fluid leakage of 1 to 10 km^3 over 10 m.y., with a 60-km-long fault providing 10 to 100 km^3 over the same period. A seismic pulse model is therefore capable of leaking substantial quantities of fluids and strongly localizing fluid flow adjacent to individual faults.

Fault zone heterogeneity and along-fault fluid flow

The foregoing discussions provide a basis for faults acting as conduits for fluid flow. However, the analysis of active flow systems, together with the localized nature of fault-controlled mineralization and mineral deposits, demonstrates that the nature of conductive fault-related fluid flow is heterogeneous. For example, flow within fractured groundwater aquifers and hydrocarbon fractured reservoirs, even within macroscopically connected fracture systems, is typified by unpredictable flow rates. These flow rates have heterogeneous and perhaps even power-law scaling characteristics, a feature attributed to the nonlinear relationships between aperture, fracture intensity, and connectivity (Nelson, 2001; Neuman, 2008; Seebeck et al., 2014). Similarly, fault-controlled geothermal and mineral deposit systems are commonly characterized by localized flow, with high-permeability pathways, such as fault zone complexities, providing the upward conduits for geothermal fluids derived from sources at much higher temperatures and greater depths (e.g., Curewitz and Karson, 1997; Sibson, 2001; Fairley and Hinds, 2004a, b; Cox, 2005). Whether these systems are fluid driven or tectonically driven, they are commonly referred to as critically stressed, in the sense that they are always near or at the point of failure (Barton et al., 1995). This is an attribute ascribed to active fault, earthquake, and conductive flow systems, and is reflected by their power-law scaling, complexity of interactions, and heterogeneity of flow (Barton et al., 1995; Cox, 2005). These characteristics mean that an active fault/fracture system can provide the sustained flow systems with localized pathways along major faults that are required to form mineral deposits. In this section, we briefly outline a quantitative model for the structure of fault zones and highlight their role as conductive pathways using constraints from Irish-type Zn-Pb deposits and a high-quality outcrop analogue from Malta.

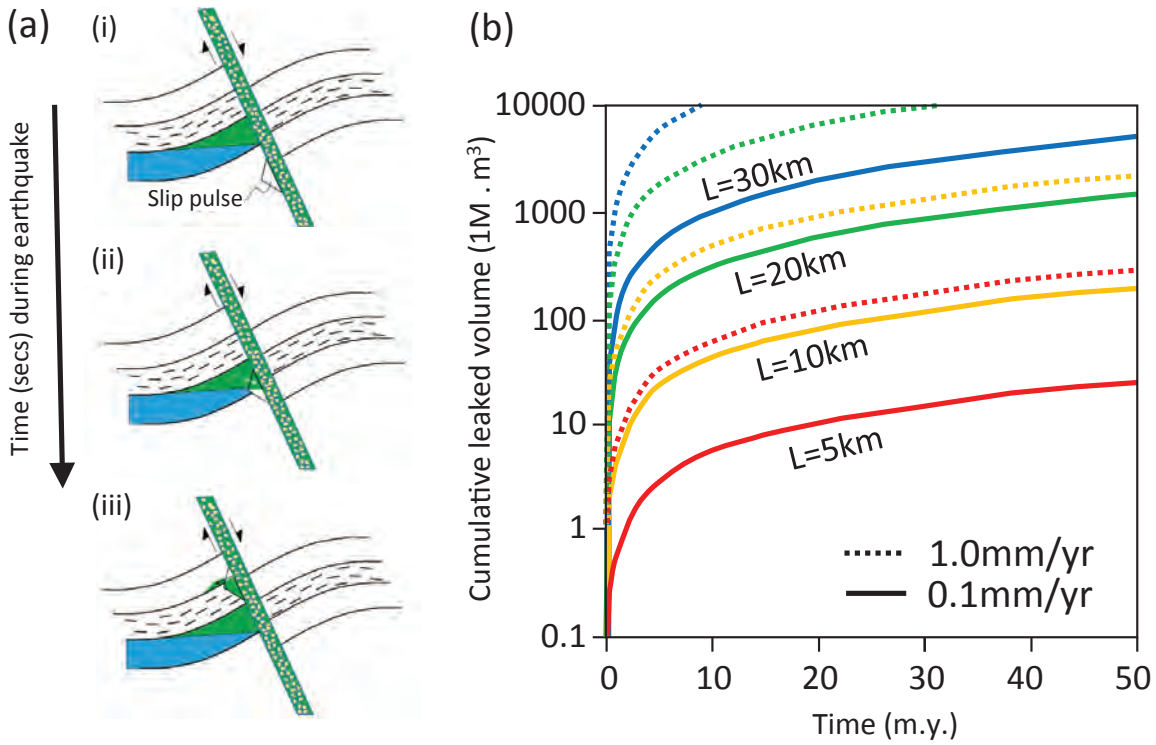

Fig. 12. (a) Schematic illustrations of transient dilation created by a slip pulse during seismic rupture. The model of Wilkins and Naruk (2007) was developed to investigate the impact of a slip pulse void (triangle) on hydrocarbon leakage (i), but it is equally applicable to formation waters to mineralizing fluids. When the void comes in contact with mobile hydrocarbons and/or formation water (not shown in diagram) within a reservoir, or host, rock (ii), these fluids leak into the void and then migrate along the fault until another area of highly permeable rock is encountered (iii), or fluid may escape to the surface. (b) Cumulative leaked volume (1 M · m^3) vs. time (m.y.) curves associated with slip-pulse activity along faults with different lengths and slip rates.

Model for fault zone structure: Whatever the nature of a given host rock, where normal faults localize and grow, they always display associated structural complexity and fault rock content and are never single planar surfaces (Fig. 5). The most important processes contributing to this complexity are propagation-related segmentation and refraction, followed by subsequent erosion of related asperities and the formation of associated minor fractures and/or faults. This deformation generates fault rock and a broad range of associated structures, all contained within what is typically called a damage zone (Caine et al., 1996; Childs et al., 1996, 2009a). Segmentation arises from the bifurcation of propagating fault surfaces to form relay zones bounded by fault segments, circumstances that are promoted by the mechanical heterogeneity of host rocks and the host-rock sequence occurring on a broad range of scales, even along a single fault (Childs et al., 2009a). Relay zones within extensional basins are marked by relay ramps that accommodate displacement transfer between overlapping segments (Peacock and Sanderson, 1991; Childs et al., 1995). Relay ramps steepen as displacement increases, with rotation and internal deformation of the ramp eventually leading to breaching of the relay and perhaps even double-breaching to form a lens (Fig. 5; Walsh et al., 1999; Childs et al., 2009a; Giba et al., 2012). Given the progressive increase in strain as a relay evolves from intact to breached and doubly breached, increasing amounts of fracturing, associated dilations, and fault rock are progressively generated from the erosion of these structures.

Childs et al. (2009a) developed a quantitative model for fault zones that reconciles the evolution of a broad range of fault zone components. The growth of fault zones was indexed to across-fault shear strain, which is the displacement to thickness ratio, in the case of fault rock and lenses, or the displacement to segment separation ratio for relays. They showed that there is a systematic increase in shear strain from intact relays through to fault rock, with characteristic ranges of shear strains for different fault zone components (Fig. 5; Childs et al., 2009a). Relays are rapidly established during the propagation of an individual fault and will have a given separation at low displacement. As displacement accumulates, a relay will increase in shear strain, migrating horizontally and to the right on a displacement vs. separation plot, because separation does not increase with growth (Fig. 5). In that sense, relays can be a precursor to localized dilations and fault rock generation, which, in turn, provide a basis for fluid flow localization. This possibility is explored in the following sections in the context of the Irish and North Pennine Zn-Pb orefields and a world-class outcrop analogue for fault zone structure.

Fault zone structure in Irish-type deposits: The importance of segmentation in the formation of mineral deposits is illustrated for the Lisheen and Silvermines Irish-type Zn-Pb deposits (Figs. 3a, 13). Irish-type deposits are considered to be a subclass of carbonate-hosted Zn-Pb deposits because they have characteristics in common with both sedimentary-exhalative (sedex) and Mississippi Valley-type (MVT)

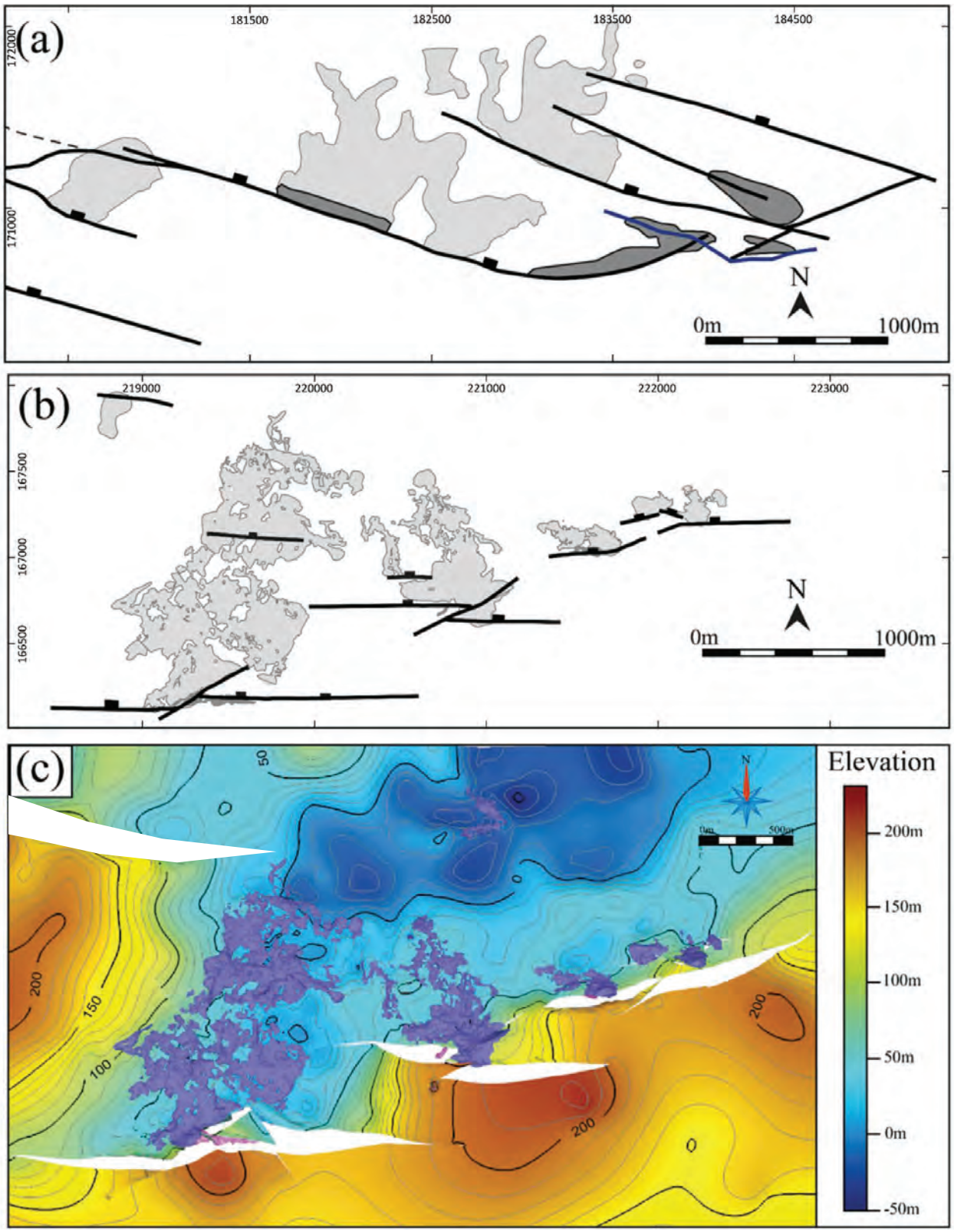

Fig. 13. Fault maps for Silvermines (a) and Lisheen (b), showing the distribution of stratiform orebodies associated with individual fault segments (light gray) and crosscutting orebodies adjacent to faults (dark gray): the latter are best developed close to branch lines or along breaching faults within Silvermines. (c) Structure contour map of base reef limestone within Lisheen, showing the main orebodies (purple) and the locations of fault polygons (normal faults are extensional and have a gap between footwall and hanging-wall cutoffs). Mineralization within footwall oolites (pink) is contiguous with that of hanging-wall reef limestones, despite the presence of the intervening bounding fault—a relationship suggesting postfaulting mineralization.

deposits (Wilkinson, 2014), with syn- through to epigenetic mineralization that is the same age as or close (<ca. 5 m.y.) to the age of the host rocks and with moderately high fluid temperatures (up to 250°C) that are distinctly different from typical MVT ores (Leach et al., 2005). As with most Irish-type deposits, mineralization in Lisheen and Silvermines is replacive and developed within the hanging walls of normal faults, with maximum displacements of 200 to 350 m, either toward the base of reef limestones as stratiform Zn-Pb orebodies or as near-fault bodies crosscutting the limestone-shale stratigraphic units (Fig. 14; Andrew, 1986, 1995; Hitzman et al., 1992; Johnston et al., 1996; Johnston, 1999). The structure of these deposits is dominated by segmentation arising from north-south Carboniferous extension applied to a lower Paleozoic basement containing east-northeast structural fabrics and structures (Johnston, 1999; Bonson et al., 2012). The effect of north-south oblique extension is the formation of arrays of predominantly left-stepping fault segments occurring on different scales (Figs. 13, 14a) attributed to bifurcation resulting from major rheological boundaries within the

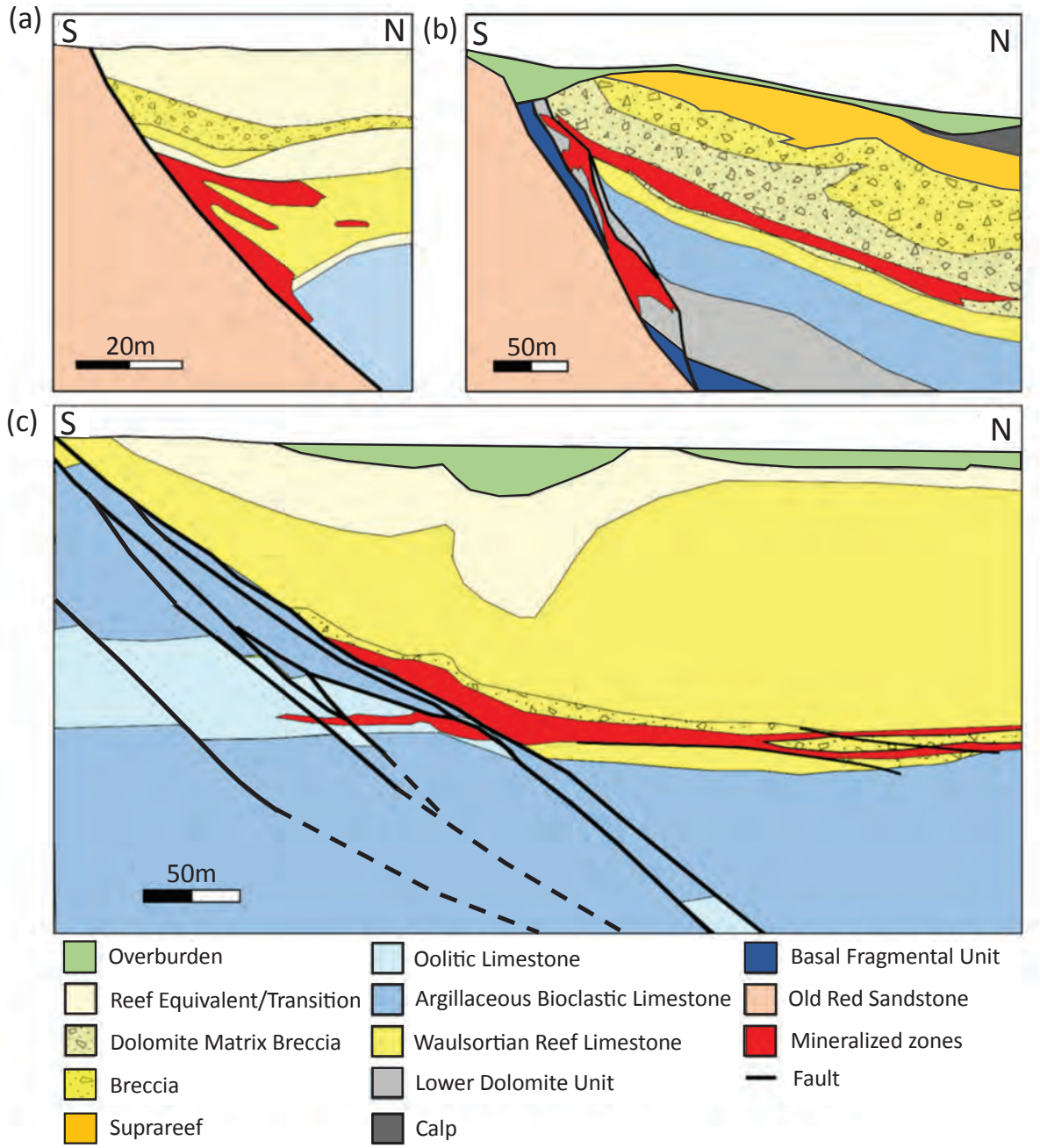

Fig. 14. Representative north-south cross sections through Waulsortian reef-hosted Irish-type deposits at (a) Tynagh (Clifford et al., 1986), (b) Silvermines (Taylor, 1984), and (c) Lisheen (Kyne et al., 2017), (c). Zn-Pb mineralization occurs as stratiform orebodies at or near the base of the Waulsortian Reef and as crosscutting orebodies adjacent to the bounding faults. The principal stratigraphic units are provided in the legend, and the scales are different for each cross section.

faulted sequence (Bonson et al., 2012; Kyne et al., 2017). Fault segments with separations of 300 to 500 m exercise a major control on the location of individual orebodies (Fig. 13). The main stratiform orebodies are associated with larger-scale segments, whereas crosscutting orebodies tend to be adjacent to the branch points (i.e., intersection points) and breaching faults of breached relays. Breached relays and related mineralization are associated with the larger displacements (~350 m) of Silvermines (Fig. 13a), with intact relays and intervening ramps preserved along the lower-displacement (~200 m) Lisheen system (Fig. 13b), a relationship that is consistent with the relay scaling shown in Figure 5 (Bonson et al., 2012).

The importance of even smaller scale complexities in Irish-type deposits is underscored by the fact that smaller-scale breached relays (with separations <~100 m) along the main fault segments, as illustrated by Lisheen (Fig. 13a), are marked by lower Zn-Pb ratios and higher concentrations of Cu, Ni, and As (Fusciardi et al., 2003)—observations that suggest they have acted as the main feeders for up-fault flow. For further details of Lisheen and Silvermines structure and mineralization, see Kyne et al. (2017) and Torremans et al. (2017). The two principal factors for smaller-scale breached relays localizing up-fault flow in these deposits are improved stratigraphic sequence connectivity and increased fracturing and brecciation. The first factor is controlled by the additional across-fault sequence juxtapositions and flow connections arising from the ramp-related deformation, and displacement variations associated with relays (Manzocchi et al., 2010). This is illustrated in Figure 15 for a very simple model in which the presence of an intact relay along a fault offsetting a sequence of interbedded permeable and impermeable units provides flow connections on a structure that would otherwise have had no across-fault flow (Fig. 15b). Although the result, in this case, is a thoroughly 3D connected flow system, even a breached relay would provide more favorable circumstances for up-fault flow given the improved juxtaposition-related connectivity. The second factor is accentuated fracturing and brecciation associated with relays and fault complexities, an issue we explore below in the context of an outcrop study of a structural analogue of Lisheen and Silvermines.

Fault zone structure-outcrop analogue: The Maghlaq fault, a normal fault with 210-m vertical displacement, defines the southern coast of Malta and the northern boundary of the Miocene-Quaternary Pantelleria Rift (Fig. 16a; Bonson et al., 2007). The faulted sequence comprises mainly limestones with an internal clay unit about 50 m thick, and excellent exposure of the fault zone permits the full range of fault zone complexity to be characterized along a 3-km-long portion of the fault (Fig. 16). The fault comprises a series of left-stepping fault segments, all of which are interpreted to be breached relays, with the resulting fault characterized by a series of bends and lenses separated by simpler fault zone structure (Bonson et al., 2007). Over much of its length, the main fault is a relatively simple structure, forming a 5- to 40-m-wide zone with two principal slip surfaces that bound deformed host rocks arranged in stratigraphic order from footwall to hanging wall.

Whereas the host-rock deformation is defined by cataclastic deformation bands and associated porosity loss, host-rock breccias and fracture zones are concentrated adjacent to fault

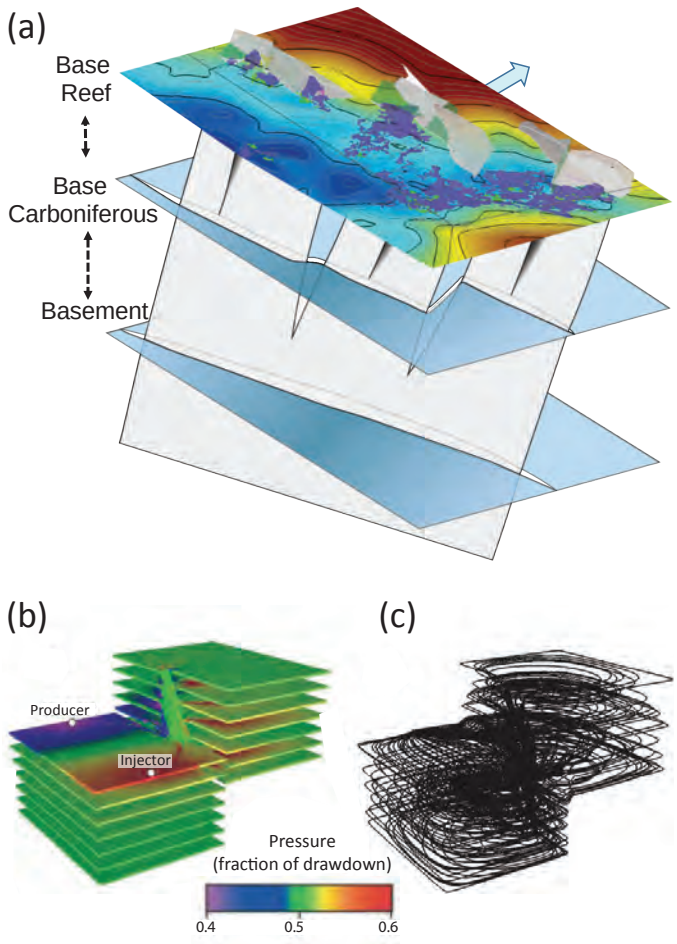

Fig. 15. (a) Schematic 3D diagram of the Lisheen deposit illustrating two depths at which segmentation occurs to form large- and small-scale fault segments. The contoured surface is the base reef limestone (see Fig. 13c), which is transected by faults (shown in gray) and contains four main orebodies (purple). (b) Model showing flow paths associated with flow within the top layer (layer 1) of the hanging-wall compartment of a multilayered, faulted model in which injector-producer pair is on the top layer (from Manzocchi et al., 2010). The model comprises a layer-cake sequence of permeable and impermeable layers, each three grid blocks thick—for the sake of clarity, only the central grid blocks of each permeable layer are shown in (b), with grid blocks colored by pressure, normalized to the total pressure difference between the injector and producer well. The model does not contain fault rock. Fault throw is 20 m, vertical exaggeration is 10, and model is 500 × 500 × 78 m. (c) Streamlines for the model in (b) showing flow paths in every permeable layer in the model. Simulation performed using 3DSL from Streamsim, and flow paths derived from its associated pressure solver (Manzocchi et al., 2010).

zone complexities, including branch lines, where fault segments intersect, and fault lenses, where host rock and/or fault rock are enclosed by slip surfaces. The major bend along the Maghlaq fault is interpreted to be a breached relay (Bonson et al., 2007). It is characterized by multiple fault lenses on a range of scales that progressively erode this bend, generating increased densities of fractures and fault rock (Figs. 16a, 17a). The branch line between the main fault and a high-angle fault adjacent to a smaller-scale fault bend is marked by a breccia zone that is up to 10 m wide and plunges along the intersection of both faults (Fig. 17c). Breccia development is accentuated because the slip direction of the minor fault was not

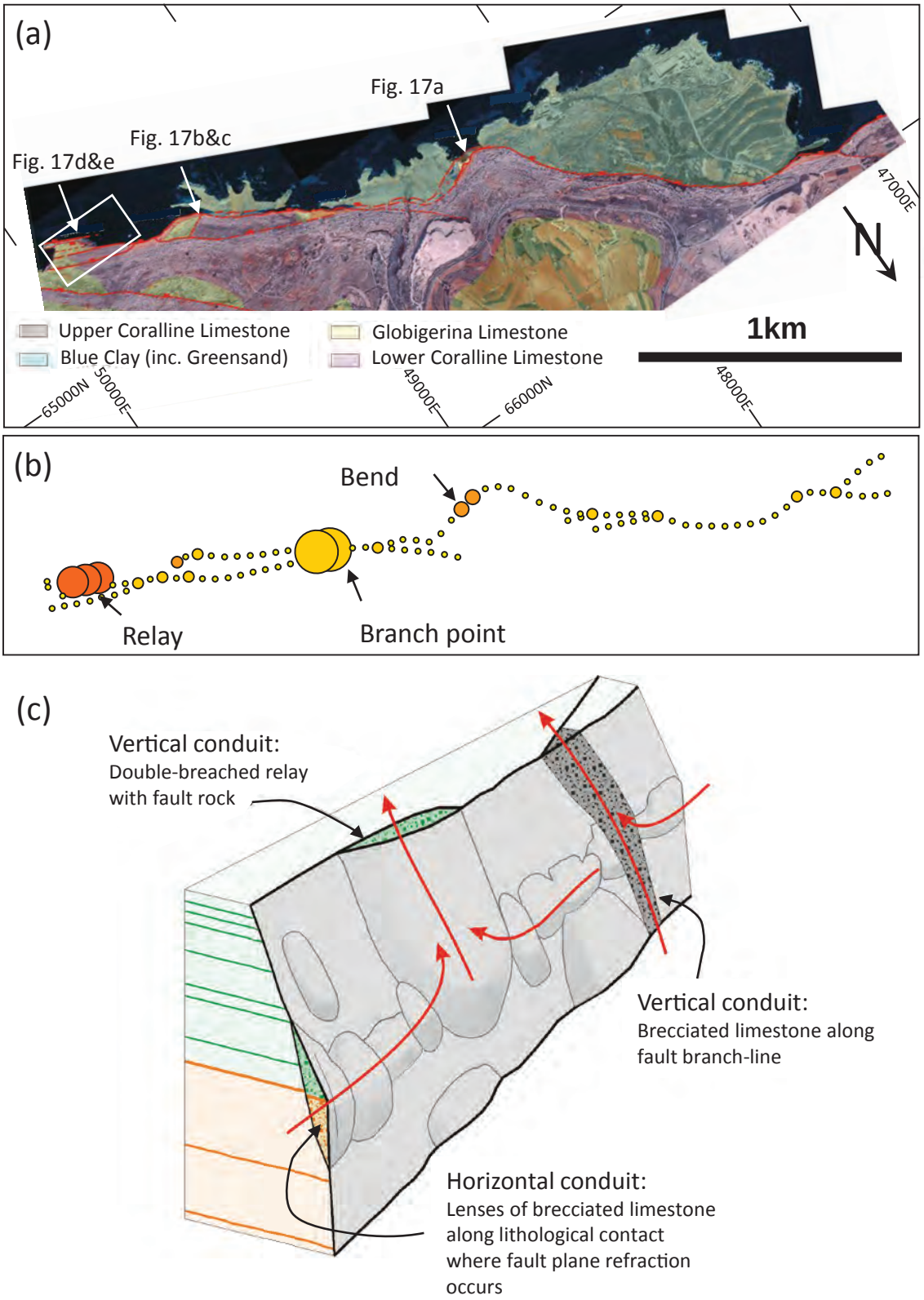

Fig. 16. (a) Map of the Maghlaq fault, Malta, which downthrows to the top of the map (north is toward the bottom right). The fault trace, shown in red, is right-stepping and comprises a number of complexities that are shown as outcrop photographs in Figure 17. The faulted sequence predominantly comprises limestones. Modified from Bonson et al. (2007). (b) Map of Maghlaq fault highlighting the fracture intensity along the fault (scale of bubbles is linked to fracture intensity). (c) Schematic diagram showing complexity of structure associated with lens arising from a double-breached relay, a branch line between two fault surfaces, and a series of lenses linked to erosion of fault refraction.

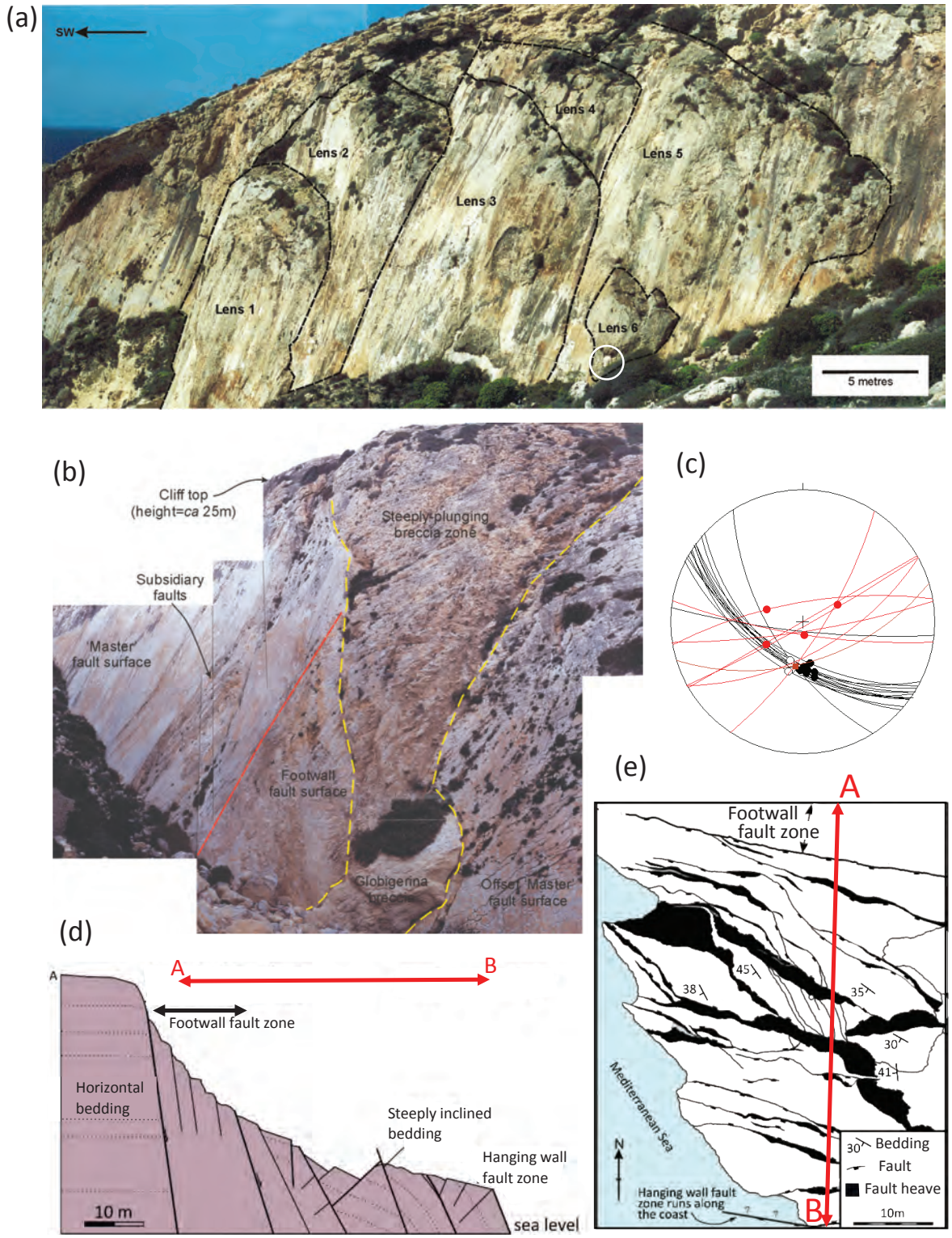

Fig. 17. (a) The Ras Hanzir fault bend on the Maghlaq fault with a view of overlapping lenses on the footwall slip surface, looking west-northwest. Fault zone lenses are annotated 1 to 7. Note the person for scale (circled). (b) Ras il-Hamrija branch line showing the intersection of a steeply plunging breccia zone. (c) Stereonet from Ras il-Hamrija branch line showing the main fault surface and slip directions (black) and the minor intersecting slip surfaces and slip directions (red). Strain incompatibility between these orientations leads to the generation of breccias. (d) Cross section of Tal-Gawwija breached relay ramp: the line of section (A-B) is shown in (e), though it extends farther to the north of map. (e) Map of the Tal-Gawwija breached relay ramp with deformation accommodated by a network of synthetic and antithetic faults that cause locally high bed dips. Toward the south of the exposure, solution erosion is intense, and the relay deformation is mapped in less detail. Fault heave shading is shown for the mapped surface, which is close to the top of the Lower Coralline Limestone (see Fig. 16).

originally parallel to either the major fault or the branch line (Fig. 17c). The associated kinematic complications appear to become progressively resolved, because the slip directions on younger subsidiary slip surfaces of the minor fault approach that of the main fault (Bonson et al., 2007).

The final example of fault zone complexities along the Maghlaq fault is a small breached relay, with a separation of 50 m, accommodating the transfer of more than 30 m of displacement at Ras il-Hamrija (Fig. 17e). The associated relay ramp has high internal bed dips, accommodating displacement transfer and shearing of the ramp down to the hanging wall (Fig. 17d), and is very heavily faulted by variably oriented internal faults. The intensity of faulting is illustrated by fault displacement populations (Fig. 18a) measured along sample lines extending from regional scale (10.8 km) down to relay scale (~50 m). All of the derived samples define an approximately straight line and, therefore, power-law, cumulative frequency vs. displacement distributions (Fig. 18a). This indicates that the fault system has self-similar, i.e., fractal, scaling properties over a few orders of magnitude of displacement (100–<0.1 m). What these data also show is that breached relays have fault intensities that are between one and two orders of magnitude higher than background fault intensities, a feature which is also consistent with progressive increases in structural heterogeneity on smaller scales. Self-similarity of structure is a fundamental characteristic of faults and earthquake systems and has major implications for heterogeneity of structure and flow.

The nature of potential flow heterogeneity can be explored for the Maghlaq fault from estimates of fault/fracture density for outcrops along the length of the fault (Fig. 16b). These show that densities are very strongly localized adjacent to fault zone complexities (Fig. 18). Furthermore, even in the absence of robust measurements of fracture or breccia apertures from the available outcrop data, the cubic flow law (eq. 2) would suggest that flow heterogeneity is likely to be much greater than the heterogeneity of fault densities. The Maghlaq fault therefore provides strong evidence for the highly localized nature of conductive up-fault flow.

Subhorizontal fault zone heterogeneity: Using outcrop examples, we have illustrated how steeply plunging branch lines, relays, bends, and lenses provide potential pathways for up-fault flow. Although these are arguably the most important flow conduits for sourcing fluids from depth, subhorizontal complexities arising from the refraction of faults through mechanically different layers (Figs. 5b, 16c) will provide a basis for lateral as well as vertical flow within fault zones. Fault dips are typically steeper in more brittle units, such as limestones and sandstones, and shallower through clays and/or shales (Fig. 5c). Refraction is only seen on smaller-scale faults adjacent to the Maghlaq fault, because their preservation potential at larger displacements is low. They are mechanically removed and incorporated as fault rock. In other fault systems, such irregularities can be the locus for dilations, with either accentuated fluid flow or even the generation of veins on the steeper portions of fault surfaces (Fig. 5b). Dunham (1934) first demonstrated that the normal faults controlling mineralization within the North Pennines Pb-Zn orefield have strongly refracting geometries. These faults act as both the flow conduits and traps for vein-hosted mineral deposits (Fig. 19c), with wider veins localized within steeper, more dilatant portions of the faults. The significance of fault refraction and related veining was reinforced by Newhouse (1942) in his classic book on structural controls and mineralization (Fig. 19c; see below).

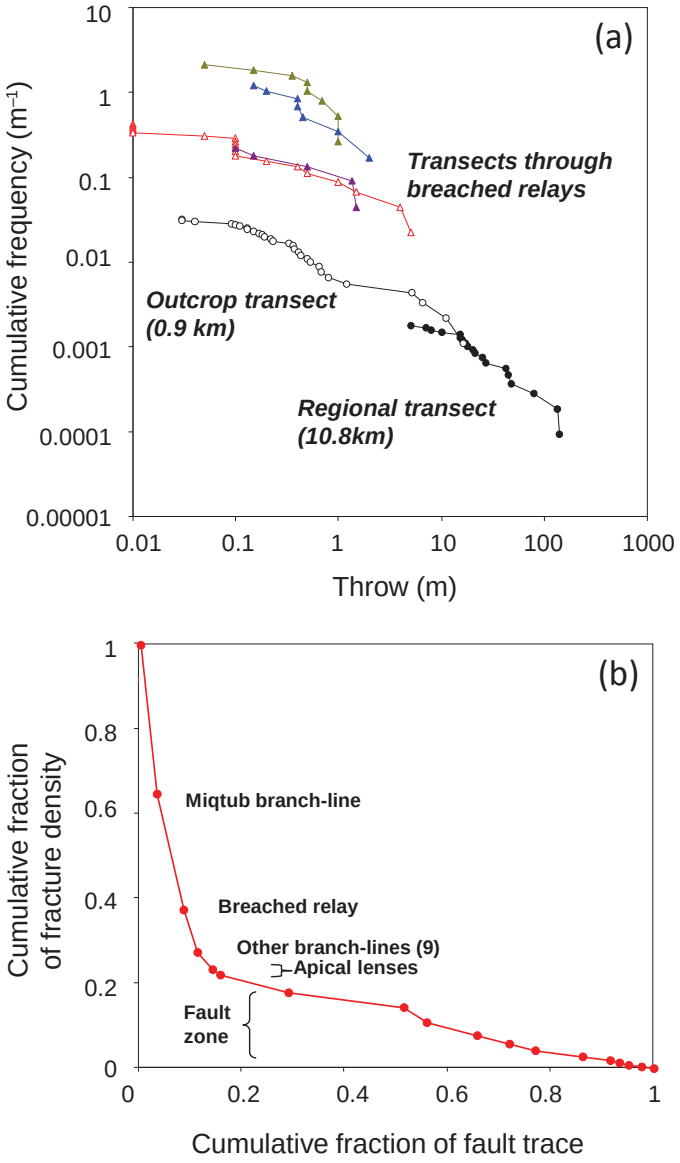

Fig. 18. (a) Fault displacement populations across the Maghlaq fault measured along different sample transects that are approximately perpendicular to fault strike. For each curve, the displacement of each fault encountered on a transect is recorded. The displacements are then ranked in decreasing order with an associated frequency of 1 through to the total number of faults; this cumulative frequency is then normalized to sample line length (in meters) to allow direct comparison of the frequencies of individual sample lines. Sample lines included a 10.8-km-long regional transect and a 0.9-km outcrop transect, which have very consistent fault populations, with straight-line power-law distributions. A selection of short line transects from within breached relays show very high fault frequencies. (b) Plot of cumulative fraction of fracture density against cumulative fraction of fault trace, showing that 80% of the Maghlaq fault trace comprises only 20% of the fracture density, with fault zone structural complexities providing most of the fracture density.

In this section, we have shown that faults are strongly heterogeneous structures, with the development of fractures and fault rock generating up-fault and along-fault complexities. A

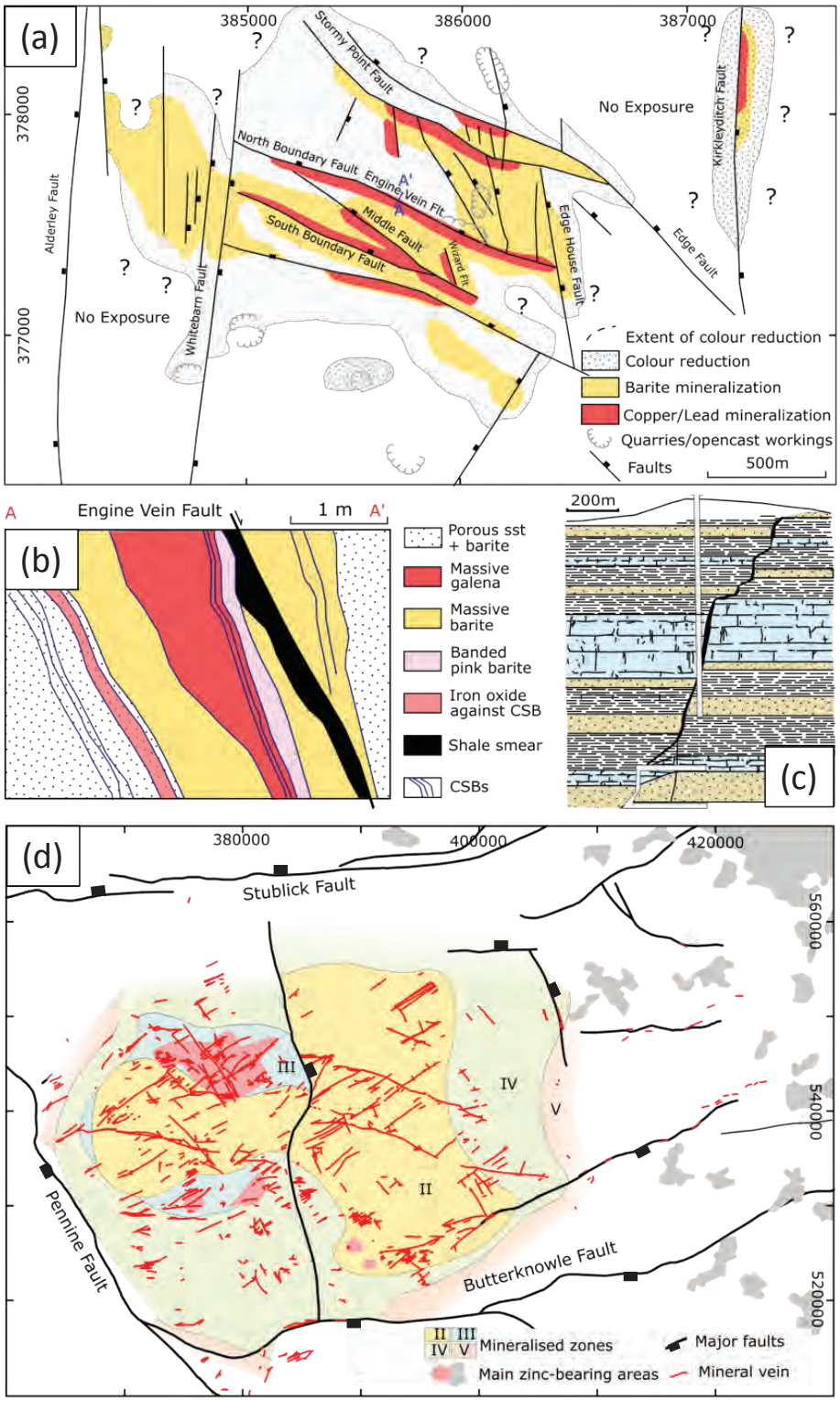

Fig. 19. (a) Map of Alderley Edge Cu-Zn-Pb-Fe mine, showing the distribution of Cu-Pb and barite relative to normal faults (Rowe and Burley, 1997). A black rectangle is shown on the downthrown (i.e., hanging-wall) side of the faults. (b) Cross section of Engine Vein fault, which is a fault rather than a vein, showing the distribution of mineralization, shale smears, and cataclastic slip bands (deformation bands), from Rowe and Burley (1997). (c) Cross section of mineralized fault from Wolfcleugh mine in North Pennines Pb-Zn orefield (Newhouse, 1942), displaying fault refraction through a limestone, sandstone, and shale sequence. Associated mineralization (black) is best developed in association with the steep fault dips developed within strong limestones (blue) and sandstones (yellow). (d) Fault map showing normal faults (black) bounding the North Pennines orefield and the main mineral veins (red). Mineralized zones are as follows: II = galena with subordinate sphalerite, III = galena-sphalerite, IV = galena, V = no sulfides (barite). Abbreviations: CSB = cataclastic slip band, flt = fault, sst = sandstone.

combination of processes, including segmentation, linkage, and refraction, is responsible for the formation of structural heterogeneities, which are typically aligned subvertically or subhorizontally within fault zones (Figs. 16c, 19c). Because of the strongly nonlinear relationship between fracture density and aperture, on the one hand, and flow localization, on the other (see eq. 2), structural complexities can become the locus for conductive flow pathways. Flow within these conductive flow systems is often strongly localized and unpredictable, with anisotropic permeability structure being the rule rather than exception. These principles underpin the importance of faults as flow-controlling structures, an issue we now explore in the context of sedimentary rock-hosted mineral deposits.

Fault-Controlled Fluid Flow and Mineralization

In the preceding sections, we have outlined generic aspects of the potential impact of faults on fluid flow from a passive to active role, in which fault-related flow is either fluid driven or tectonically driven. Here we show how faults and their associated processes can have a variety of effects on the geometry, location, and origin of mineral deposits, with particular reference to Zn-Pb and Cu sedimentary rock-hosted mineral deposits. These effects are considered in the context of contrasting end-member issues and are illustrated using case studies from basins that have had relatively little later metamorphism and deformation.

Fault-controlled flow: Sealing vs. conduits

Earlier sections have highlighted the principal controlling factors on the nature of fault-related fluid flow. Here we illustrate the difference between faults acting as seals or conduits using examples of sedimentary rock-hosted Zn-Pb sulfide deposits from the North Pennines and East Irish Sea Basin orefields. Spatiotemporal and genetic links between these orefields have not been advocated by previous work, but there are compelling grounds for suggesting they may be related, both geometrically and temporally, even though the impact of faults on mineralization is very different.

The East Irish Sea Basin, together with its adjacent margins, including the Cheshire Basin, is a petroleum province containing extensive and varied mineralization, including sandstone-hosted Cu-Pb-Zn-Fe deposits and fault-related diagenetic cementation of Middle to Late Triassic age (see Rowe and Burley, 1997, and references therein). Alderley Edge is a Cu-Pb-Zn-Fe deposit formed within the Alderley horst, a 3-km-wide, N-S–oriented Triassic high bounded by approximately 300 m displacement faults. This horst provides a larger-scale focus for fluid flow with the trapping of barite and iron-reducing fluids in a 1-km-wide area (Fig. 19). Within this trap, sulfide mineralization lies in the immediate footwalls of N- to NNW-oriented normal faults, with displacements of approximately 10 to 20 m, and is hosted within the relatively porous Sherwood sandstones, the principal reservoir for the East Irish Sea hydrocarbon basin. Mineralization is postfaulting and replacive, rather than vein hosted, and is localized adjacent to zones of cataclastic deformation bands and shale smears (Fig. 19). The presence of a rhombohedral network of faults is attributed to the complex crosscutting nature of approximately N-S trending Permo-Triassic faults and the internal deformation of the Alderley horst. On a more regional scale, ENE-trending normal faults within 25 km to the south and west of this area are parallel to and believed to be reactivated equivalents of early Carboniferous normal faults that extend directly along strike into the Welsh Zn-Pb orefield.

The North Pennine Pb-Zn orefield is developed within an approximately 25 × 25 km horst overlying the Weardale Granite, bounded by km-scale displacement normal faults (Fig. 19d), with the Permian to Triassic NNW-striking Pennines fault in the west and the ENE-striking Stublick and Butterknowle faults in the south and north, both of which were active during early Carboniferous extension and were subsequently reactivated in Permian to Triassic times (Fig. 19d; Bouch et al., 2006). On the large scale, this orefield is also defined by barite as the dominant gangue mineral beyond the main sulfide deposits and fluorite as the main gangue mineral adjacent to the deposits. Mineralization is developed within rhombohedral fault-related vein systems, with the best sulfide mineralization associated with ENE-trending normal faults and, to a lesser extent, NNW-trending normal faults; occasional relatively long east-west veins are poorly mineralized sinistral strike-slip faults (Fig. 19). Fault refraction through the strongly lithified and well-cemented limestone-sandstone-shale sequences provided dilations and associated mineral veins, particularly adjacent to the stronger mechanical units (i.e., limestones; Fig. 19c). These are classic fault-related vein deposits (Dunham, 1934; Newhouse, 1942), and the most recent estimates of their timing is Late Permian to end Triassic (Bouch et al., 2006).

Even though the available evidence suggests that the timing and configuration of normal faulting in the North Pennines orefield are similar to those of the East Irish Sea and Cheshire basins, the nature of fault-controlled mineralization is very different. In one case, faults within porous host-rock sequences are barriers to flow but nevertheless guide fluids along their immediate footwalls. In the other case, faults within lithified sedimentary sequences act as conduits for up-fault flow—behavior that is entirely consistent with their mechanical and hydraulic properties. The underlying source of Zn-Pb-Cu mineralizing fluids is not known, but it is, of course, tempting to suggest they may be the remobilized equivalent of underlying early Carboniferous Irish-type deposits or derived from the same basement source. These hypotheses should be investigated by future research.

Expression of mineralization: Basement vs. basin expression

It is rarely possible to examine the nature of mineralization at different depths within a given mineral province, a situation that is compounded in some cases, such as the Zambian Copperbelt, by later metamorphism and deformation. Evidence from different areas within the U.K. and Ireland associated with the early Carboniferous Zn-Pb orefield provides some constraints on how fault-controlled mineralization develops in associated basement rocks. Existing models for Irish-type mineral deposits suggest that Zn-Pb is mainly scavenged from Ordovician basement rocks previously deformed during the Caledonian/Acadian orogenies, or from older crystalline rocks, now unconformably overlain by early Carboniferous sequences (for further details, see Wilkinson, 2003, 2014; Wilkinson and Hitzman, 2015). These basement source rocks

cannot be investigated in the Midlands of Ireland, principally because the level of exposure rarely incises deep enough. However, directly across the Irish Sea, the Ordovician and Silurian metasedimentary basement rocks of Wales contain vein-hosted Zn-Pb deposits, which were the subject of Phillips' (1972) classic work on fault-related valving and hydraulic fracturing, referred to earlier (Fig. 9).

The Zn-Pb vein-hosted deposits of Wales are developed along, and kinematically related to, post-Caledonian ENE-striking normal faults with displacements of up to ~1 km (Ashton, 1981; Fitches, 1987). Combined with estimates of burial depths of up to ~8 km and field relations and dating suggesting an early Carboniferous age (Fitches, 1987), these constraints collectively suggest that these vein deposits could be the underlying basement-hosted equivalents of now eroded Zn-Pb Irish-type deposits in Wales. Similar vein-hosted Zn-Pb ore is found in basement rocks in Ireland (Everett et al., 1999; Wilkinson, 2010), but they are not as laterally extensive as their Welsh equivalents and were developed at much shallower depths (<~1 km). This depth difference is consistent with the very different nature of the associated deposits. The Welsh vein-hosted deposits display the characteristics of a strongly overpressured hydrothermal system developed at km-scale depths within the seismogenic (i.e., earthquake-prone) upper crust.

The classic Irish-type deposits of Lisheen and Silvermines developed at much shallower depths (<500 m) than contemporaneous Welsh vein-hosted deposits. They are characterized by stratiform hydrothermal breccias and karst-related dissolution, which together provide a more stratigraphically extensive and bacterially and/or seawater-influenced mineralized system (Figs. 13, 14; Wilkinson and Hitzman, 2015). Strong fluid connectivity between basement and basin would have been provided by normal faults penetrating deep within the crust. Displacement-length scaling of faults suggests that even faults with relatively low maximum displacements, equivalent to those bounding Irish-type deposits (>200 m), will penetrate deep into the underlying brittle basement and transect the entire seismogenic zone (to depths of ~10 km: Walsh and Watterson, 1988). This scenario is supported by a recent review of European basin-hosted base metal deposits (Muchez et al., 2005), which concluded that fluids with evaporated seawater signatures migrated downward through sedimentary basins into basement rocks, potentially residing there for up to tens of millions of years. Subsequently, the metal-bearing fluids were tapped from the basement and expelled along normal faults to form Zn-Pb deposits hosted by overlying carbonate rocks as well as the Cu deposits of the Kupferschiefer in southwest Poland.

Geometric configuration of orebodies: Stratiform vs. crosscutting

Whether epigenetic deposits are stratiform or not depends on many factors, the most important of which is the receptive or nonreceptive nature of the host-rock sequence, a characteristic that is linked to the intrinsic porosity-permeability properties, reactive nature, or chemical makeup of the host rock. Here we are exclusively concerned with the structural controls on orebody geometry, which we briefly consider for Irish-type deposits.

An important characteristic of many major deposits in the Irish Zn-Pb orefield is the presence of laterally persistent stratiform dolomitic breccias within the hanging wall of major feeder faults. At Lisheen and Silvermines, for example, ore mineralization is typically replacive of dolomitic hydrothermal breccias that are localized at the base of reef, adjacent to the rheological interface between the reef and underlying shale-limestone sequence (Fig. 14; Andrew, 1986, 1995; Hitzman et al., 1998; Wilkinson, 2003; Fusciardi et al., 2003). Wilkinson et al. (2011) attribute these breccias to dissolution and replacement of diagenetic dolomites during subseafloor hydrothermal fluid flow at shallow depths (<150 m). Their formation during active faulting and their localization within the hanging walls of bounding faults are consistent with models for normal faults indicating that near-surface hanging-wall deformation is marked by fracturing and dilatations even along subhorizontal interfaces (Zhang and Sanderson, 1996). Near-surface mineralization and the presence of associated karst-dissolution structures are consistent with the seawater-derived bacteriogenic sulfur isotopic signature of these stratiform deposits (Fusciardi et al., 2003; Wilkinson et al., 2005). Even though the development of stratiform orebodies is a feature of all economic Irish-type deposits, it is unclear why dolomitic breccias and stratiform deposits, with significant spatial footprints, are developed adjacent to some faults and not others; this is the subject of ongoing research.

Nonstratiform orebodies in the Irish Zn-Pb orefield are restricted to within and adjacent to their bounding feeder fault. Associated mineralization has a more hydrothermal isotopic signature and is spatially associated with lenses of host rock/fault rock and accentuated faulting/fracturing of the immediate hanging-wall limestone sequence (Kyne et al., 2017). These orebodies are particularly well developed within the Silvermines deposit adjacent to and along relay breaches and branch lines (Fig. 13a). By contrast to stratiform deposits, which are strongly influenced by host-rock lithological units and associated breccia development, crosscutting orebodies are controlled by fault-related damage.

Fault-related deformation: Syngenetic vs. epigenetic?

Faults not only represent the conduits and barriers associated with mineral systems but, if they are active during sedimentation, also are responsible for the accommodation space and facies changes of the sediments that host mineral deposits. Deformation associated with the Basin and Range province and the North Sea shows that hanging-wall subsidence and footwall uplift are capable of providing the geometric and stratigraphic configurations so commonly associated with deposits (Figs. 2, 10). Whereas fault-related stratigraphic thickness changes are typical of synsedimentary growth faults emerging at the contemporary free surface, equivalent trap configurations are not, as is locally suggested, an indicator of syngenetic mineralization. Instead, the synsedimentary architecture, with associated heterogeneous and ponded facies variations, can represent the host-rock configuration for later epigenetic mineralization (Fig. 20a). Here we present examples illustrating this principle and show that faults acting as conduits for mineralizing fluids and extending from depth toward the surface can show both

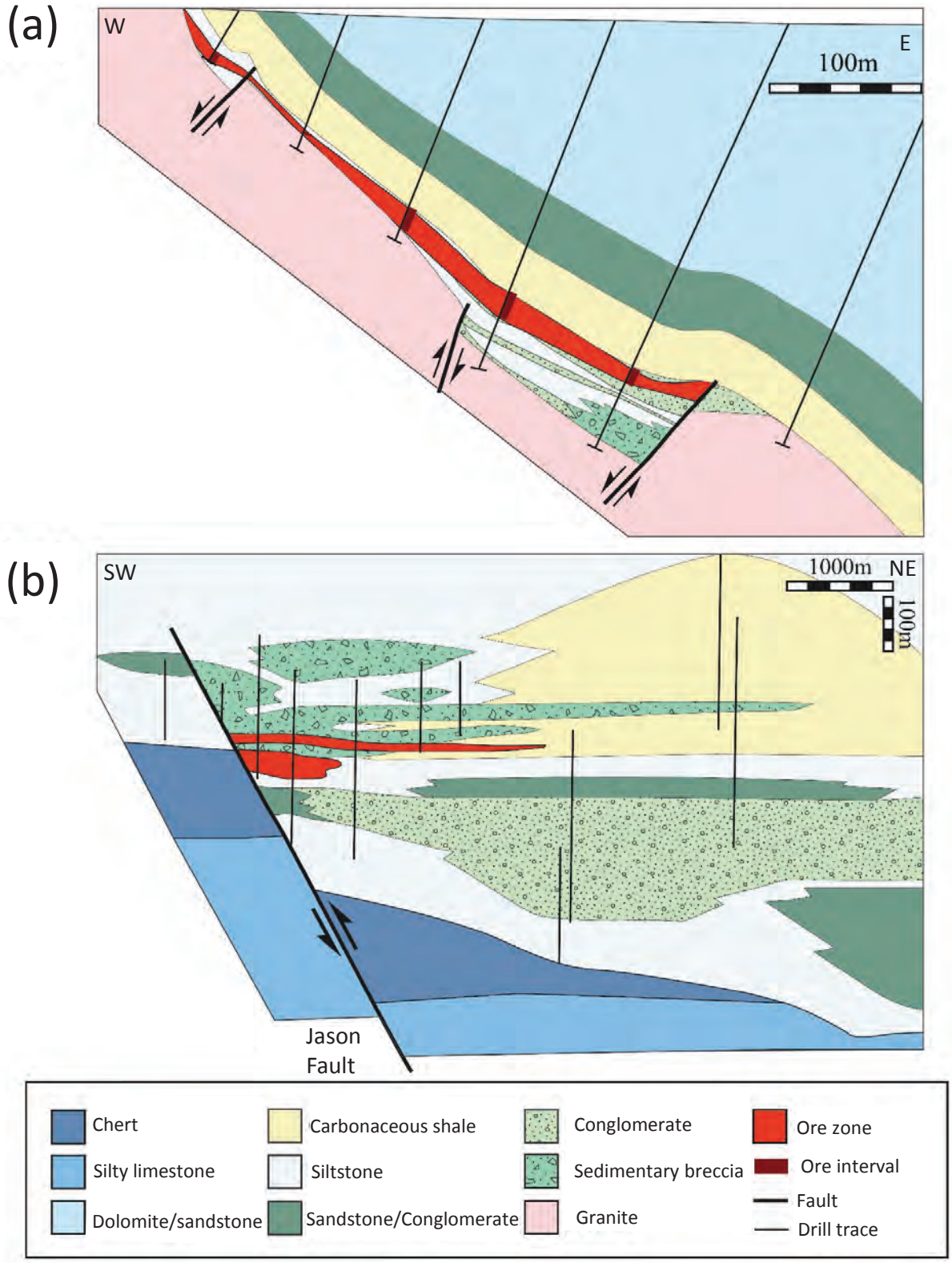

Fig. 20. (a) Cross section through the sandstone-hosted Mwambashi B deposit in the Zambian Copperbelt (modified from Selley et al., 2005); see legend for lithologies. The section highlights the effect of a syndepositional half-graben fault on the distribution of sedimentary facies within the lower sandstone units of the Mindola Clastics Formation. This unit is then capped by a carbonaceous shale, the Copperbelt Orebody Member, which represents an effective seal below which copper-cobalt ore mineralization occurs. (b) Cross section through the Jason stratiform Zn-Pb-barite deposit, Selwyn Basin, Canada (Turner, 1990). The section, which is reconstructed from borehole data (black lines), highlights the syndepositional nature of the main bounding fault, the Jason fault, and the associated hanging-wall mineralization.

epigenetic and syngenetic signatures, whatever their spatiotemporal configuration.

Syngenetic deposits can be established on textural, mineralogical, and lithological grounds, perhaps supporting a vent complex origin overlying a feeder. In the absence of strong evidence, however, the ponding of mineral deposits, particularly within the hanging wall of faults, can locally be taken as the critical evidence favoring a sedex style of mineralization. The classic model for the Selwyn Basin (Canada) is that mineralization was synsedimentary, with sulfide and barite precipitation from a stratified, euxinic water column adjacent to a submarine exhalative plume (Goodfellow and Lydon, 2007). The geometric configuration of the Jason Zn-Pb-barite deposit is consistent with a syngenetic origin and, therefore, an equivalent age to the host rock, because mineralization is localized in the hanging wall of a normal fault showing significant across-fault sequence growth (Fig. 20b; Goodfellow et al., 1993; Leach et al., 2005). Recent work has shown, however, that Zn-Pb mineralization within this deposit postdates diagenetic barite and pyrite and is therefore epigenetic and replacive of the synfaulting host rocks (Magnall et al., 2016). By contrast, the Mwambashi B deposit in the Zambian Copperbelt, a mineralized half-graben bounded by a normal fault and directly overlain by a postfaulting carbonaceous shale cap (Fig. 20a), has always been considered to be a postfaulting epigenetic trap (Fig. 20a; Selley et al., 2005). Mwambashi B is attributed to postfaulting preferential mineralization of the hanging walls of normal faults, particularly where displacement transfer between faults has led to structural complexity and dilation (Fig. 21b; Selley et al., 2005). The Chambishi SE deposit also has an epigenetic origin, in which orebodies coincide with footwall pinch-outs in subbasins bounded by growth faults, a configuration that is attributed to mineralization of a synfaulting sequence (Fig. 21a; Selley et al., 2005).

Whereas the foregoing examples are all epigenetic deposits associated with synfaulting stratigraphic traps, some deposits have mineralization of both syngenetic and epigenetic origin, a scenario that is perhaps not surprising given the conductive nature of faults from depth up to the surface. The Silvermines Zn-Pb deposit (Fig. 19b) provides evidence for an early, mainly pyritic phase, which is syngenetic, followed by the main Zn-Pb mineralization of epigenetic origin, forming replacive stratiform bodies and fault-parallel, crosscutting zones within the host-rock carbonate-shale sequences (Andrew, 1986, 1995; Kyne et al., 2017; Torremans et al., 2017). At Lisheen, however, similar stratiform bodies of pyrite and later Zn-Pb mineralization are entirely epigenetic (Fig. 19c; Carboni et al., 2003; Fusciardi et al., 2003). On geometric grounds it might appear that Lisheen exhibits characteristics similar to those of some exhalative deposits, with mineralization and associated brecciation developed in topographic lows adjacent to individual fault segments, and not extending up associated relay ramps (Fig. 14a). This is not, however, a synsedimentary signature, and is instead attributed to the sinking and accumulation of high-density brines toward the base of the host-rock reef limestones, where bacteria can precipitate sulfides (Torremans et al., 2017).

The above discussion highlights similar geometric configurations of syngenetic and epigenetic deposits, reinforcing the notion that these fault-related origins are not mutually exclusive, either spatially or temporally, but they are to be expected. Given that the spatiotemporal window for the formation of epigenetic deposits along a fault is much longer, the preponderance of epigenetic Zn-Pb and Cu sedimentary rock-hosted deposits over syngenetic is not surprising. Another, perhaps related phenomenon is the gradual change in emphasis from earlier sedex models to a predominantly epigenetic origin for the Zn-Pb deposits in Ireland (Wilkinson and Hitzman, 2015) and the Selwyn Basin (Goodfellow et al., 1993; Magnall et al., 2016).

Mineralization: Synfaulting vs. postfaulting

Much of the literature on fault-related fluid flow advocates tectonically driven, active fault displacements at the same time as mineralization—circumstances that are consistent with all three of the fault models described: seismic pumping, seismic pulsing, and fault valving. Valve-like behavior along faults can, however, be entirely fluid pressure driven with no requirement for contemporaneous movement on adjacent faults. Similarly, the sealing nature of faults within sedimentary basins does not require active faulting and may even be better preserved during the postrift phase of basin evolution, as is typically the case for hydrocarbon fault traps. In that sense, faults can have an impact on flow well beyond the period in which they were tectonically active. For typical rifts such as the North Sea Jurassic or Irish Carboniferous, the phase of active rifting was only ca. 10 m.y., whereas the associated faults existed for at least 140 m.y. afterward and have clearly had an impact on flow (e.g., Fig. 2). Because fault valving and sealing can develop in postfaulting times, we suggest that, in individual cases, consideration should always be given to both a postfaulting and synfaulting origin for mineral deposits.

Of the several deposits already described in this paper, half are postfaulting. Zinc-Pb mineralization within the Lisheen deposit, for example, is both epigenetic and postfaulting (Fig. 19c; Carboni et al., 2003; Fusciardi et al., 2003), a spatiotemporal history that is supported by two observations: (1) the continuity of mineralization between hanging-wall reef limestones and footwall oolites, despite the intervening bounding fault (Fig. 13; Sevastopulo and Redmond, 1999), and (2) the replacive nature of mineralization across intradeposit faults (Fig. 22c; Carboni et al., 2003; Fusciardi et al., 2003). Despite a postfaulting timing for mineralization, it is possible and perhaps even likely that the formation of Lisheen is synrifting. This timing is plausible insofar as rift evolution typically involves the initiation of many faults at the early stages of rifting, with displacements gradually localizing onto fewer and bigger faults. Many faults within a basin, particularly the smaller ones, will become inactive in displacement terms, even though they can play an active role within the basinal flow system. Mineralization could, therefore, postdate movement on the Lisheen fault but still be synrift and contemporaneous with movement on other, larger basinal faults (i.e., km-scale, rather than 200-m, displacements). The Alderley Edge Cu-Zn-Pb-Fe deposit is also postfaulting and replacive, with mineralization localized adjacent to zones of cataclastic deformation bands and shale smears (Fig. 19). Field relations suggest that associated fault zones acted as passive pathways for mineralizing

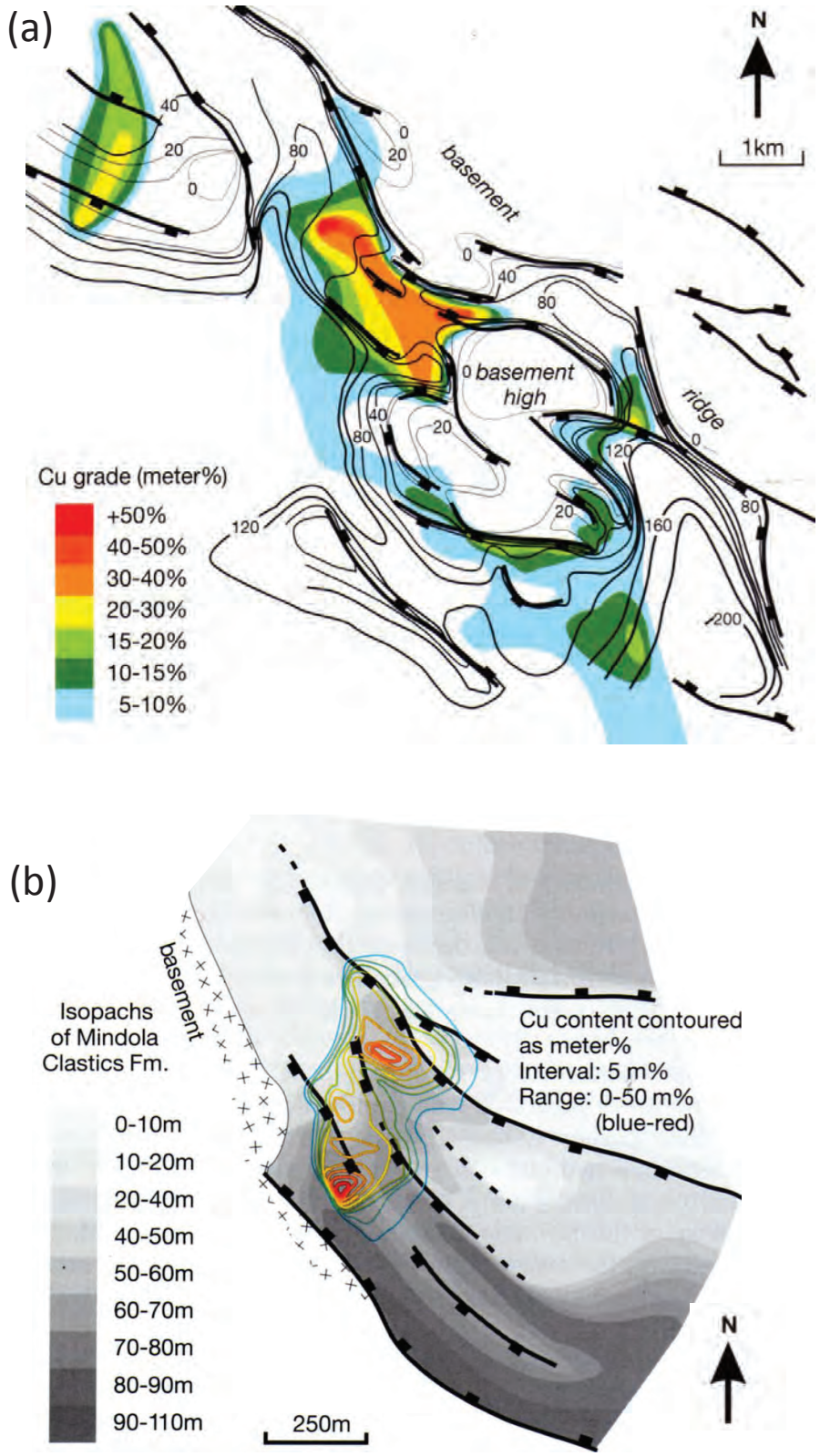

Fig. 21. Maps of (a) the Chambishi SE deposit and (b) the Mwambashi B deposit in the Zambian Copperbelt from Selley et al. (2005). Figures show surface contour projections of meter isopachs of the thickness of the Mindola Clastics Formation, the basal red-bed sequence, and faults. (a) A complex set of subbasins in the Chambichi SE deposit is formed by the intersection of NNW- and WNW-trending faults. The highest-grade areas of mineralization are bound by fault zones that controlled deposition and facies of the Mindola Clastics Formation. (b) High-grade ore in the Mwambashi B deposit is restricted to a complex set of narrow zones where faults transfer displacement.

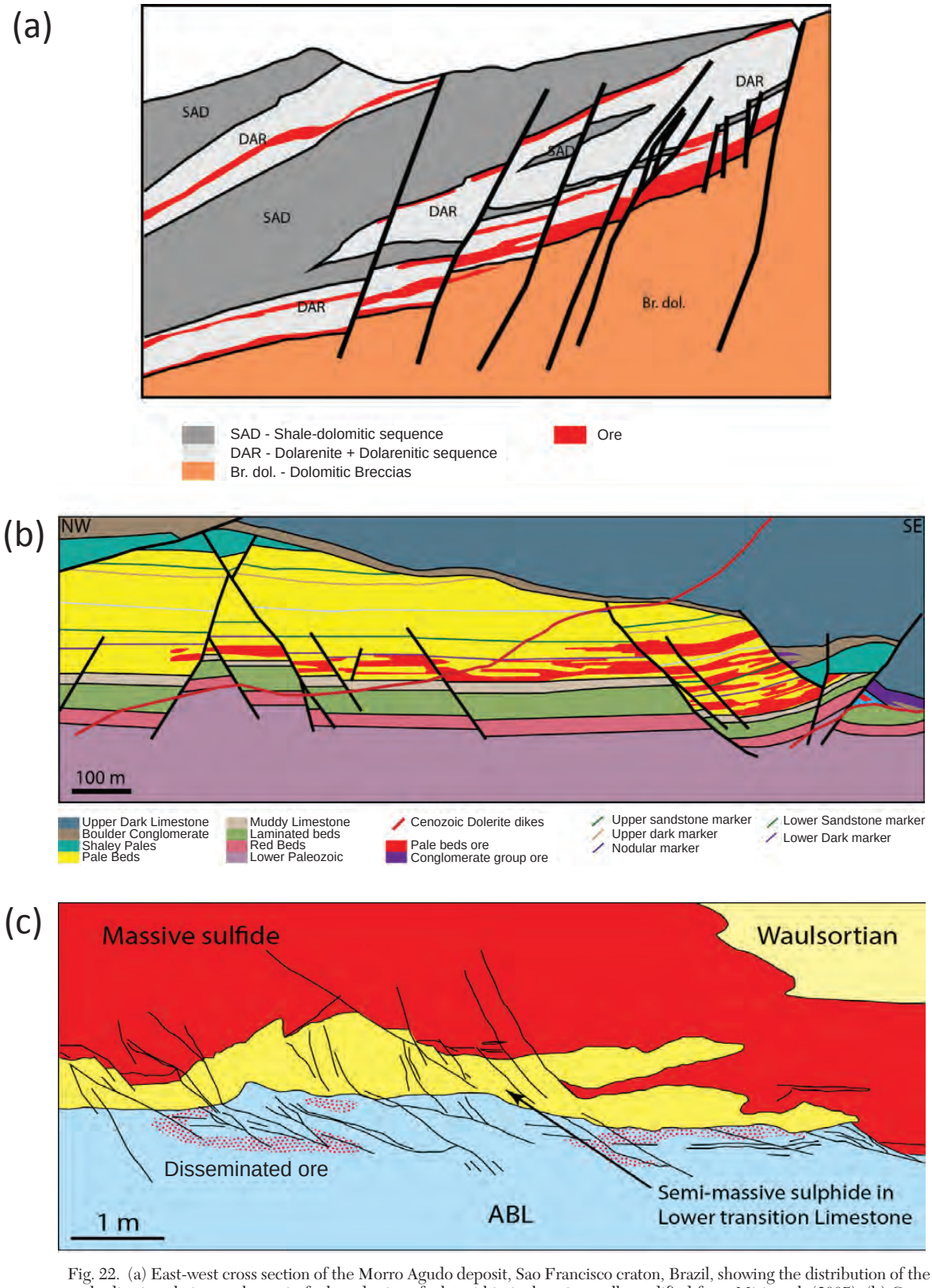

Fig. 22. (a) East-west cross section of the Morro Agudo deposit, Sao Francisco craton, Brazil, showing the distribution of the orebodies in relation to the main fault and minor faults within its hanging wall, modified from Misi et al. (2005). (b) Cross section of the Navan deposit (Ashton et al., 2015) showing the distribution of Zn-Pb mineralization within the Pale Beds host. (c) Mine face drawing from Lisheen mine (Carboni, oral commun., 2004) showing how massive and semimassive sulfides entirely postdate small-scale normal faults within the hanging wall of the main Lisheen bounding fault. The Waulsortian reef limestones (pale yellow) are the main host rock for mineralization, and they are underlain by poorly mineralized limestones and shales (blue) of the Argillaceous Bioclastic Limestone (ABL).

fluids mainly within the footwalls of faults (Rowe and Burley, 1997). Finally, the Chambishi SE and Mwambashi B deposits of the Zambian Copperbelt also postdate normal faulting, with mineralization believed to be much later than rifting, though perhaps contemporaneous with basin inversion (Figs. 20a, 21; Selley et al., 2005).

The mineral deposits we have already described in this paper reinforce the importance of postfaulting fluid flow for some mineral deposits. In the remainder of this section, we consider the distinction between syn- and postfaulting fluid flow by examining the nature of trapping within a hydrocarbon reservoir (Poui field, Trinidad) and two Zn-Pb sedimentary rock-hosted mineral deposits (Navan, Ireland; Morro Agudo, Brazil). Fluid flow associated with the hydrocarbon reservoir entirely postdates faulting and provides a trap configuration that has similarities with those of the mineral deposits. Detailed consideration of the fault geometry and mineralization of the mineral deposits, informed by the hydrocarbon reservoir geometries, favors a late or postfaulting timing for mineralization rather than a more conventional synfaulting interpretation.

Hydrocarbon reservoir: Multiple hydrocarbon fault traps in multilayered sequences locally form complexly stacked reservoirs arising from the 3D nature of postfaulting fill-spill hydrocarbon flow systems (Fig. 23; Gibson, 1994). This is illustrated for the Poui field in the Columbus Basin, Trinidad, which comprises fault traps developed within approximately 30 sandstone reservoir units. Fault sealing arises from the juxtaposition of sands and shales, and from the development of shale smears within fault zones; trapping requires in excess of 25% shale within the faulted sequence (Gibson, 1994). Hydrocarbon migration is buoyancy driven, with migration within sandstone units combining with across- and up-fault leakage. The final distribution of traps is complex, with occasional traps showing the same across-fault hydrocarbon contacts and most traps defining separate, apparently unrelated contacts, on cross sections. The migration of mineralizing fluids is also typically buoyancy driven, with chemically reactive mineralization potentially providing an even more complex flow system than hydrocarbons. Hydrocarbon flow systems are therefore very instructive insofar as they provide complex trap system geometries arising from 3D flow pathways in faulted sequences, even in circumstances where fluid migration entirely postdates faulting.

Navan Zn-Pb deposit, Ireland: Much of the mineralization in the largest Irish Zn-Pb deposit at Navan is concentrated in the footwall of the major Navan fault, which has a displacement in excess of 3 km (Ashton et al., 2015). Available evidence indicates that mineralization is syn- through to postfaulting on the scale of the entire deposit (Blakeman et al., 2002). In the footwall of the main bounding faults of the Navan deposit (Fig. 22b), the precise temporal relationship between some minor normal faults (<100-m displacement) and mineralization is, at least on geometric grounds, not as clear. These faults show no evidence of synsedimentary faulting at the time of deposition of the host-rock Pale Beds, and they clearly predate the overlying boulder conglomerates, which are marked by substantial amounts of erosion and postdate at least some of the mineralization. Two main features suggest a postfaulting age: (1) the continuous nature of some orebodies across faults and (2) the very different stratigraphic localization of ore either side of individual faults. It is possible that mineralization started in late-faulting and extended into postfaulting times, but, from the geometric configuration shown in Figure 22b, another plausible explanation is that the mineralization entirely postdates movement on the minor faults concerned. These minor faults could, for example, have ceased moving before mineralization and simply provided cross-fault pathways for connecting different units in 3D and/or acted as a valve for mineralizing fluids (Fig. 22b). Progressive localization of displacements onto larger basinward faults (to the southeast in Fig. 22b), with mineralization sourced from greater depths by those still active faults, would provide a rationale for the death of footwall minor faults and a postfaulting mineralization relationship. The important issue that a postfaulting model needs to explain is the differing stratigraphic levels of mineralization across some faults—a feature that, on an individual cross section, may appear to require faulting that is synchronous with mineralization. Flow systems are not, however, cross-sectional, but are instead thoroughly 3D, and, within a fault system comprising multiple faults with variable displacements, associated changes in fault rock distributions and cross-fault juxtapositions can produce very complex 3D flow pathways and mineralization distributions. Geometric similarities between hydrocarbon traps within the Poui field and the mineral traps associated with some of the minor faults contained within the footwall of the main Navan fault provide some support for a postfaulting origin with migration involving across-fault flow and sealing, together with up-fault valving. Future detailed structural and textural analysis of the minor footwall faults is, however, required to establish whether they ceased moving before the still active main deposit-bounding faults provided the principal conductive pathways for mineralization.

Morro Agudo Zn-Pb deposit, Brazil: A mineral system interpreted to be syn- to postfaulting but showing the geometric hallmarks of postfaulting mineralization is derived from the Proterozoic sedimentary rock-hosted Zn-(Pb) deposits of the Sao Francisco craton, Brazil (Misi et al., 2005). A cross section of the Morro Agudo deposit indicates an array of normal faults within the hanging wall of a major fault that is believed to be the main feeder to the deposit (Fig. 22a). With all of the within-deposit faults showing constant along-fault cross-sectional displacements and no across-fault thickness changes, they must be postsedimentary structures, with mineralization being epigenetic in origin. The continuity of some stratiform deposits that transect individual faults indicates that the mineralization is partly or perhaps entirely postfaulting (Fig. 22a). Both explanations are plausible, but, in the absence of mine-scale structural analysis, the simplest model is a postfaulting origin with 3D mineralization pathways. That model is supported by the observation that the within-deposit faults have very small displacements (up to 10 m) relative to the scale of the 1.5-km-wide deposit, making it very likely that they will vary in displacement and even die out laterally. The variable juxtapositions would therefore provide a system that is much more connected in 3D than in cross section, providing tortuous and yet connected pathways which could entirely postdate faulting.

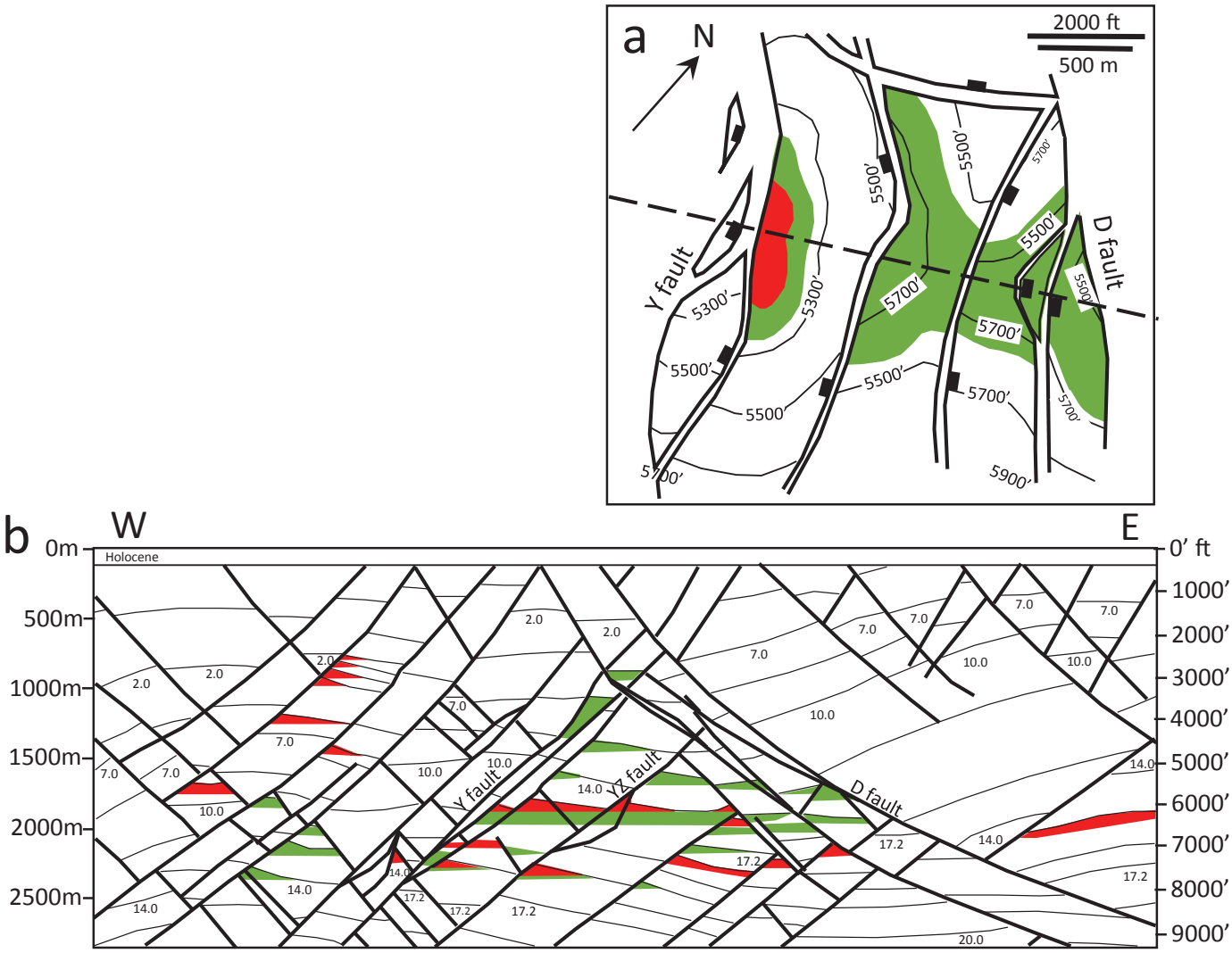

Fig. 23. Map (a) and cross section (b) showing the main faults and associated hydrocarbon traps (oil = green, gas = red) of the Poui field, Trinidad. Hydrocarbon migration is buoyancy driven and marked by 3D tortuous flow paths, with fault trapping dominated by sequence juxtaposition or membrane seals, with the latter produced by cataclastic shale smears (i.e., shaley gouge). (a) Contour map of 14-0 sandstone in central part of field. Light lines are contours (interval = 200 ft [61 m]); heavy lines are fault traces. (b) Cross section of the field with line of section along dashed line on map (a). Small numbers identify certain reservoir intervals and the three main faults are labeled (Y, YZ, and D). Modified from Gibson (1994).

Many of the deposits presented in this paper were generated by flow systems that postdate normal faulting. In common with hydrocarbon reservoirs, relatively complex distributions of traps do not require synfaulting mineralization but can instead be reconciled with postfaulting 3D flow systems. The late timing of mineralization relative to fault movement is not unexpected insofar as fault-related conductive flow can be driven by fluid pressures, leading to either passive flow or fault valving during the synrift or postrift phase of basin evolution. Given that most faults become inactive during rifting, with activity localizing onto progressively larger faults, mineralization that postdates the activity of individual faults could still be synchronous with continued basin extension when the hydrodynamics of basins benefits from high heat flows and from seismic pumping and pulsing associated with faults that are still active. Whatever the precise timing of mineralization, consideration of the 3D nature of flow can support a relatively simple postfaulting origin rather than the more familiar synfaulting models often advocated in the literature.

Impact of Faults on Basin-Scale Flow—Summary Discussion

Crustal extension provides some of the key ingredients for mineral provinces, including heat, source of brines, fault-related flow pathways, and a variety of processes driving fluid flow. Our consideration of the main processes and factors controlling fluid flow within sedimentary basins highlights the importance of normal faults as both conduits and seals for the migration and trapping of mineralizing fluids. Faults provide the essential fluid pathways connecting basement or basinal sources to sediment-hosted deposits and can play both a passive and an active role in driving fluid movement. Here

we briefly summarize how fault-related processes and drives combine to provide a sustainable flow system capable of generating mineral deposits within sedimentary basins.

The onset of rifting is marked by basin subsidence and an increase in geothermal gradient, conditions that are responsible for the emergence of a fundamental driver of basinal fluid flow: an increase in pore fluid overpressure with depth. Progressive sediment loading and disequilibrium compaction lead to the overpressuring of pore fluids, usually beginning at depths of between 500 m and ~3 km, depending on the nature of the faulted sequence. At greater depths, dissolution, cementation, and increasing temperatures lead to further overpressuring. Associated compartmentalization of basin overpressures, with substantial increases in fluid pressure toward basin centers, is attributed to normal faults with clay-rich fault rocks forming lateral seals to out-of-basin fluid flow. In these circumstances, up-fault flow provides the principal means of relieving overpressures and is a critical component of a sustainable convective flow system.

The major shortcoming of an entirely overpressured system is that there is only a finite source of fluids, with no apparent means of replenishing the system. However, a selection of fault-related processes can contribute to the cycling of fluid flow, with the expulsion of fluids arising from up-fault flow and the infiltration of fluids accommodated by down-fault flow. Four processes have been described in this paper: up-fault passive flow, fault valving, seismic pumping, and seismic pulsing.

Faults within siliciclastic and carbonate sequences containing clay and silt interbeds can comprise fault rocks which have along-fault permeabilities that are greater than the vertical permeability of the host-rock sequence (K_v). These faults may be sealing to across-fault flow within aquifers, but they can still represent effective pathways for passive upward and downward flow. At higher overpressures, up-fault flow will be accommodated by fault valving, a fluid-driven process leading to fault failure and, locally, earthquake triggering. Fault valving is accompanied by an instantaneous decrease in overpressure and perhaps even a short-term return to hydrostatic conditions, either within a fault or in adjacent stratigraphic units. Valving events can, therefore, temporarily open the system with the ingress of fluids, particularly denser brines from shallower depths. The scale of fluid mobilization by the stress cycling of valving events is uncertain, but previous studies have attributed this mechanism to the generation of vein-hosted gold deposits.

Seismic pumping associated with the earthquake cycle is capable of driving and replenishing substantial volumes of fluids. Coseismic strain associated with individual earthquakes on normal faults can lead to the upward fluid expulsion of up to ~1 km^3 from km-scale depths during large earthquakes (e.g., 0.3 km^3 for an M6.9 earthquake), with up to ~1,000 km^3 over the lifetime of a fault. Between seismic events, a rock volume extends either by dilations of fractures or by poroelasticity—strains that are porosity generating and of the same order as associated coseismic volume changes (km^3). These interseismic strains do not exist within dead basins or even within active strike-slip or reverse fault systems. It is at this time that the ingress of fluids and denser brines will occur, by either lateral or down-fault flow. Given the scale of some faults, it is therefore possible that individual faults could provide pathways for both downward and upward flow at different times and/or places. The depth of penetration of replenishing fluids will depend on many factors, including the 3D structural/stratigraphic basin configuration, the nature and timing of episodic activity on multiple faults, and the natural drives of the hydrologic system. Seismic pulsing is another process that could accommodate up- and down-fault fluid migration. Associated fluid flow arises from along-fault coseismic slip-related dilation and a suction-pump effect, which could, in principle, provide for fluid expulsion and ingress along the same fault on a scale of up to ~100 km^3 over the lifetime of a large normal fault. Taken together, seismic pumping and pulsing are therefore capable of driving and cycling substantial volumes of fluid—conditions that will promote the emergence of convective flow systems during the synrift phase of basin evolution.

The final ingredient for the generation of mineral deposits is the sourcing of brines, an important chemical constituent of mineralizing fluids permitting the scavenging of metals from either basement or lower basinal sequences. Brines can be derived from basinal sediments, particularly the evaporitic deposits toward the base of synrift sequences, and from down-fault migration of seawater. Recent work suggests that the sinking of cold but relatively dense brines from the Earth's surface does not require faults (Koziy et al., 2009). However, the presence of conductive faults within sedimentary basins provides ideal pathways for the infiltration of fluids into deeper metalliferous source rocks (Koziy et al., 2009). Relief changes associated with faulted basins, with uplifted and eroded footwalls and basin margins, provide km-scale hydraulic heads that will further accentuate the downward migration of brine-rich fluids into basinal sequences and underlying basement. If, as Holm (1998) has suggested, pore fluid pressures within the faulted and fractured basement rocks underlying basins are hydrostatic (e.g., Holm, 1998), the continuous source of brines to great depths is very likely, even in the absence of active crustal extension.

A variety of mainly fault related issues and processes contribute to the formation of sediment-hosted mineral deposits. Insights and models from earthquake, hydrocarbon, and mineral studies indicate that fault-controlled flow systems in sedimentary basins are capable of cycling large volumes of fluids through the crust. The sinking of dense brines and the rise of hot hydrothermal solutions are facilitated by the passive and active role of normal faults in the migration of fluids during the synrift and postrift phases of basin evolution. The emergence of convective flow provides a sustainable flow system capable of generating mineral deposits, at least until crustal extension-related thermal and tectonic drives decline and/or the source is depleted.

Conclusions

Insights and models derived from earthquake, hydrocarbon, and mineral studies show that normal faults can have a major impact on basinal flow within rift basins by acting as barriers to lateral flow and/or as conduits to up- or down-fault flow. This duality of flow behavior, which can show spatiotemporal variations even on the scale of individual faults, exercises a major control on basinal flow. Faulting can actively drive fluid flow by a variety of associated processes, including seismic

pumping and pulsing, and provide a means of driving substantial volumes of fluids ('00 km^3 on km displacement faults) during individual coseismic slip events. The expulsion of fluids during earthquakes is followed by longer interseismic periods of extension and dilation of host rocks with an associated replenishment of fluids—earthquake-related processes that, together, contribute to the convection of basinal fluids. Faults nevertheless continue to have an impact on fluid flow even after they have become tectonically inactive during the late synrift or postrift phases of basin evolution. Faults can act as lateral seals to out-of-basin flow, contributing to the buildup and compartmentalization of basin overpressures and to the migration and trapping of fluids. They still represent the most effective conduits for the upward flow of overpressured and hydrothermal fluids and for the downward sinking of heavy brines, either by fault valving or by acting as passive flow pathways. Flow heterogeneity along faults, arising from along-fault structural complexities, provides a basis for the thoroughly 3D flow systems that localize fluid flow and lead to the formation of mineral deposits. Consideration of the broad range of fault-related processes suggests that fault systems within rifts contribute to the emergence and support of sustainable, crustal-scale convective flow systems on the scale required for the formation of mineral deposits and provinces.

Acknowledgments

This paper has emanated from research that is supported in part by a research grant from Science Foundation Ireland (SFI) under grant number 13/RC/2092 and co-funded under the European Regional Development Fund. Part of the work of KT was carried out for the European Union's Horizon 2020 Research and Innovation Programme under Marie Skłodowska-Curie grant agreement number 745945. The authors would like to thank Vedanta Resources and the Geological Survey Ireland for providing data. Helpful reviews from Jim Evans, John Swenson, and Jeff Mauk are much appreciated and significantly improved this paper. Thanks also to Maptek, Paradigm, Mira Geoscience, Aranz Geo (now Seequent), and Midland Valley for our use of their software. We are also grateful to Peter Haughton for producing Figure 3b.

REFERENCES

Allan, U.S., 1989, Model for hydrocarbon migration and entrapment within faulted structures: AAPG Bulletin, v. 73, p. 803–811.

Andrew, C.J., 1986, The tectono-stratigraphic controls to mineralization in the Silvermines area, County Tipperary, Ireland, *in* Andrew, C.J., Crowe, R.W.A., Finlay, S., Pennel, W.M., and Pyne, J.F., eds., Geology and genesis of mineral deposits in Ireland: Dublin, Irish Association for Economic Geology, p. 377–417.

——1995, The Silvermines district, Co. Tipperary, Ireland: Society of Economic Geologists Guidebook Series, v. 21, p. 247–258.

Ashton, J.H., 1981, Wallrock geochemistry and ore geology of certain mineralised veins in Wales: Ph.D. thesis, Aberystwyth, University of Wales, 357 p.

Ashton, J.H., Blakeman, R.J., Geraghty, J.F., Beach, A., Coller, D., Philcox, M.E., Boyce, A.J., and Wilkinson, J.J., 2015, The giant Navan carbonate-hosted Zn-Pb deposit: A review, *in* Archibald, S.M., and Piercey, S.J., eds., Current perspectives on zinc deposits: Dublin, Irish Association for Economic Geology, p. 85–122.

Barton, C.A., Zoback, M.D., and Moos, D, 1995, Fluid flow along potentially active faults in crystalline rock: Geology, v. 23, p. 683–686.

Bence, V.F., and Person, M.A., 2006, Faults as conduit-barrier systems to fluid flow in siliciclastic sedimentary aquifers: Water Resources Research, v. 42, p. 1–18, doi: 10.1029/2005WR004480.

Berg, S.S., 2004, The architecture of normal fault zones in sedimentary rocks: Analysis of fault core composition, damage zone asymmetry, and multiphase flow properties: Ph.D. thesis, Bergen, Norway, University of Bergen, 118 p.

Blakeman, R.J., Ashton, J.H., Boyce, A.J., Fallick, A.E., and Russell, M.J., 2002, Timing of interplay between hydrothermal and surface fluids in the Navan Zn + Pb orebody, Ireland: Evidence from metal distribution trends, mineral textures, and $\delta^{34}S$ analyses: Economic Geology, v. 97, p. 73–91.

Blundell, D.J., 2002, The timing and location of major ore deposits in an evolving orogen: The geodynamic context: Geological Society, London, Special Publication 204, p. 1–12.

Bonson, C.G., Childs, C., Walsh, J.J., Schöpfer, M.P.J., and Carboni, V., 2007, Geometric and kinematic controls on the internal structure of a large normal fault in massive limestones: The Maghlaq fault, Malta: Journal of Structural Geology, v. 29, p. 336–354.

Bonson, C., Walsh, J.J., and Carboni, V., 2012, The role of faults in localising mineral deposits in the Irish Zn-Pb orefield, *in* Vearncombe, J., ed., Structural geology and resources 2012: Kalgoorlie, Australian Institute of Geologists (AIG), p. 8–11.

Bouch, J.E., Naden, J., Shepherd, T.J., McKervey, J.A., Young, B., Benham, A.J., and Sloane, H.J., 2006, Direct evidence of fluid mixing in the formation of stratabound Pb-Zn-Ba-F mineralisation in the Alston block, North Pennine orefield (England): Mineralium Deposita, v. 41, p. 821–835.

Boullier, A.M., and Robert, F., 1992, Palaeoseismic events recorded in Archaean gold-quartz vein networks, Val d'Or, Abitibi, Quebec, Canada: Journal of Structural Geology, v. 14, p. 161–179.

Caine, J.S., Evans, J.P., and Forster, C.B., 1996, Fault zone architecture and permeability structure: Geology, v. 24, p. 1025–1028.

Carboni, C., Walsh, J.J., Stewart, D.R.A., and Güven, J.F., 2003, Timing and geometry of normal faults and associated structures at the Lisheen Zn/Pb deposit—investigating their role in the transport and the trapping of metals, *in* Eliopoulos, D.G., et al., eds., Proceedings of the Seventh Biennial SGA Meeting, Mineral Exploration and Sustainable Development: Rotterdam, Millpress Science Publishers, p. 665–668.

Childs, C., Watterson, J., and Walsh, J.J., 1995, Fault overlap zones within developing normal fault systems: Journal of the Geological Society, London, v. 152, p. 535–549.

——1996, A model for the structure and development of fault zones: Journal of the Geological Society, London, v. 153, p. 337–340.

Childs, C., Manzocchi, T., Nell, P.A.R., Walsh, J.J., Strand, J.A., Heath, A.E., and Lygren, T.H., 2002, Geological implications of a large pressure difference across a small fault in the Viking graben: Norwegian Petroleum Society, Special Publication 11, p. 127–139.

Childs, C., Walsh, J.J., Manzocchi, T., Strand, J., Nicol, A., Tomasso, M., Schöpfer, M.P.J., and Aplin, A., 2007, Definition of a fault permeability predictor from outcrop studies of a faulted turbidite sequence, Taranaki, New Zealand: Geological Society, London, Special Publication 292, p. 235–258.

Childs, C., Manzocchi, T., Walsh, J.J., Bonson, C.G., Nicol, A., and Schöpfer, M.P.J., 2009a, A geometric model of fault zone and fault rock thickness variations: Journal of Structural Geology, v. 31, p. 117–127.

Childs, C., Sylta, Ø., Moriya, S., Morewood, N., Manzocchi, T., Walsh, J.J., and Hermanssen, D., 2009b, Calibrating fault seal using a hydrocarbon migration model of the Oseberg Syd area, Viking graben: Marine and Petroleum Geology, v. 26, p. 764–774.

Clifford, J.M., Ryan, P., and Kucha, H., 1986, A review of the geological setting of the Tynagh orebody, Co. Galway, *in* Andrew, C.J., Crowe, R.W.A., Finlay, S., Peynele, W.M., and Pyne, J.F., eds., Geology and genesis of mineral deposits in Ireland: Dublin, Irish Association for Economic Geology, p. 419–440.

Cox, S.F., 2005, Coupling between deformation, fluid pressures, and fluid flow in ore-producing hydrothermal systems at depth in the crust: Economic Geology 100th Anniversary Volume, p. 39–75.

Cox, S.F., Sun, S.-S., Etheridge, M.A., Wall, V.J., and Potter, T.F., 1995, Structural and geochemical controls on the development of turbidite-hosted gold quartz vein deposits, Wattle Gully mine, central Victoria, Australia: Economic Geology, v. 90, p. 1722–1746.

Cox, S.F., Braun, J., and Knackstedt, M.A., 2001, Principles of structural control on permeability and fluid flow in hydrothermal systems: Reviews in Economic Geology, v. 14, p. 1–24.

Curewitz, D., and Karson, J.A., 1997, Structural settings of hydrothermal outflow: Fracture permeability maintained by fault propagation and interaction: Journal of Volcanology and Geothermal Research, v. 79, p. 149–168.

Dunham, K.C., 1934, The genesis of the North Pennine ore deposits: Quarterly Journal of the Geological Society, v. 90, p. 689–720.
Everett, C.E., Wilkinson J.J., and Rye D.M., 1999, Fracture-controlled fluid flow in the lower Palaeozoic basement rocks of Ireland: Implications for the genesis of Irish-type Zn-Pb deposits: Geological Society, London, Special Publication 155, p. 247–276.
Fairley, J.P., and Hinds, J.L., 2004a, Rapid transport pathways for geothermal fluids in an active Great Basin fault zone: Geology, v. 32, p. 825–828.
——2004b, Field observation of fluid circulation patterns in a normal fault system: Geophysical Research Letters, v. 31, L19502, doi: 10.1029/2004GL020812.
Fisher, Q.J., and Knipe, R.J., 2001, The permeability of faults within siliciclastic petroleum reservoirs of the North Sea and Norwegian continental shelf: Marine and Petroleum Geology, v. 18, p. 1063–1081.
Fitches, B., 1987, Aspects of veining in the Welsh Lower Palaeozoic Basin: Geological Society, London, Special Publication 29, p. 325–342.
Fossen, H., Schultz, R.A., Shipton, Z.K., and Mair, K., 2007, Deformation bands in sandstone: A review: Journal of the Geological Society, London, v. 164, p. 755–769.
Fristad, T., Groth, A., Yielding, G., and Freeman, B., 1997, Quantitative fault seal prediction: A case study from Oseberg Syd: Norwegian Petroleum Society, Special Publication 7, p. 107–124.
Fusciardi, L.P., Güven, J.F., Stewart, D.R.A., Carboni, V., and Walsh, J.J, 2003, The geology and genesis of the Lisheen Zn-Pb deposit, Co. Tipperary, Ireland, *in* Kelly, J.G., Andrew, C.J., Ashton, J.H., Boland, M.B., Earls, G., Fusciardi, L., and Stanley, G. eds., Europe's major base metal deposits: Dublin, Special Publication of the Irish Association for Economic Geology, p. 455–282.
Gaarenstroem, L., Tromp, R.A.J., de Jong, M.C., and Brandenburg, A.M., 1993, Overpressures in the central North Sea; implications for trap integrity and drilling safety, *in* Parker, J.R., ed., Petroleum Geology of Northwest Europe: Proceedings of the 4th Conference: London, Geological Society, p. 1305–1313.
Giba, M., Walsh, J.J., and Nicol, A., 2012, Segmentation and growth of an obliquely reactivated normal fault: Journal of Structural Geology, v. 39, p. 253–267.
Gibson, R.G., 1994, Fault-zone seals in siliciclastic strata of the Columbus Basin, offshore Trinidad: AAPG Bulletin, v. 78, p. 1372–1385.
Goodfellow, W.D., and Lydon, J.W., 2007, Sedimentary exhalative (sedex) deposits: Geological Association of Canada, Mineral Deposits Division, Special Publication 5, p. 163–183.
Goodfellow, W.D., Lydon, J.W., and Turner, R.J.W, 1993, Geology and genesis of stratiform sediment-hosted (sedex) zinc-lead-silver sulphide deposits: Mineral deposit modeling: Geological Association of Canada, Special Paper 40, p. 201–251.
Grueschow, E., Kwon, O., Main, I.G., and Rudnicki, J.W., 2003, Observation and modeling of the suction pump effect during rapid dilatant slip: Geophysical Research Letters, v. 30, 4 p., doi: 10.1029/2002GL015905.
Guéguen, Y., and Dienes, J., 1989, Transport properties of rocks from statistics and percolation: Mathematical Geology, v. 21, p. 1–13.
Hitzman, M.W., O'Connor, P., Shearley, E., Schaffalitzky, C., Beaty, D., Allan, J.R., and Thompson, T., 1992, Discovery and geology of the Lisheen Zn-Pb deposit, Rathdowney Trend, Ireland, *in* Bowden, A.A., Earls, G., O'Connor, P.G., and Pyne, J.F., eds., The Irish minerals industry 1980–1990: Dublin, Irish Association for Economic Geology, p. 227–246.
Hitzman, M.W., Allan, J.R., and Beaty, D.W., 1998, Regional dolomitization of the Waulsortian limestone in southeastern Ireland: Evidence of large-scale fluid flow driven by the Hercynian orogeny: Geology, v. 26, p. 547–550.
Hitzman, M.W., Selley, D., and Bull, S., 2010, Formation of sedimentary rock-hosted stratiform copper deposits through Earth history: Economic Geology, v. 105, p. 627–639.
Holm, G., 1998, How abnormal pressures affect hydrocarbon exploration and exploitation: Oil and Gas Journal, v. 96, p. 79–84.
Johnston, J.D., 1999, Regional fluid flow and the genesis of Irish Carboniferous base metal deposits: Mineralium Deposita, v. 34, p. 571–598.
Johnston, J.D., Coller, D., Millar, G., and Critchley, M.F., 1996, Basement structural controls on Carboniferous-hosted base metal mineral deposits in Ireland: Geological Society, London, Special Publication 107, p. 1–21.
Jolley, S.J., Barr, D., Walsh, J.J., and Knipe, R.J., 2007a, Structurally complex reservoirs: Geological Society, London, Special Publication 292, 491 p.
Jolley, S.J., Dijk, H., Lamens, Q.J., Fisher, Q.J., Manzocchi, T., Eikmans, H., and Huang, Y., 2007b, Faulting and fault sealing in production simulation models: Brent province, northern North Sea: Petroleum Geoscience, v. 13, p. 321–340.
King, G.C.P., Stein, R.S., and Rundle, J.B., 1988, The growth of geological structures by repeated earthquakes. 1. Conceptual framework: Journal of Geophysical Research: Solid Earth, v. 93, p. 13,307–13,318.
Knipe, R.J., 1992, Faulting processes and fault seal: Norwegian Petroleum Society, Special Publication 1, p. 325–342.
Koziy, L., Bull, S., Large, R., and Selley, D., 2009, Salt as a fluid driver, and basement as a metal source, for stratiform sediment-hosted copper deposits: Geology, v. 37, p. 1107–1110.
Kristensen, M.B., Childs, C.J., Olesen, N.Ö., and Korstgard, J.A., 2013, The microstructure and internal architecture of shear bands in sand-clay sequences: Journal of Structural Geology, v. 46, p. 129–141.
Kyne, R., Torremans, K., Doyle, R., Güven, J., and Walsh, J., 2017, Segmented fault arrays and their control on the formation of Irish-type Zn-Pb deposits: Society for Geology Applied to Mineral Deposits, 14th Biennial SGA Meeting, Quebéc City, Canada, August 20–23, 2017, Proceedings, p. 617–620.
Leach, D., Sangster, D., Kelley, K., Large, R.R., Garven, G., Allen, C., Gutzmer, J., and Walters, S.G., 2005, Sediment-hosted lead-zinc deposits: A global perspective: Economic Geology 100th Anniversary Volume, p. 561–607.
Lehner, F.K., and Pilaar, W.F., 1997, On a mechanism of clay smear emplacement in synsedimentary normal faults: Norwegian Petroleum Society, Special Publication 7, p. 39–50.
Lindsay, N.G., Murphy, F.C., Walsh, J.J., and Watterson, J., 1993, Outcrop studies of shale smears on fault surfaces: International Association of Sedimentologists, Special Publication 15, p. 113–123.
Lothe, A.E., Sylta, Ø., Lauvrak, A., and Sperrevik, S., 2006, Influence of fault map resolution on pore pressure distribution and secondary hydrocarbon migration; Tune area, North Sea: Geofluids, v. 6, p. 122–136.
Magnall, J.M., Gleeson, S.A., Stern, R.A., Newton, R.J., Poulton, S.W., and Paradis, S., 2016, Open system sulphate reduction in a diagenetic environment—isotopic analysis of barite ($\delta^{34}S$ and $\delta^{18}O$) and pyrite ($\delta^{34}S$) from the Tom and Jason Late Devonian Zn-Pb-Ba deposits, Selwyn Basin, Canada: Geochimica et Cosmochimica Acta, v. 180, p. 146–163.
Manzocchi, T., Walsh, J.J., Nell, P.A.R., and Yielding, G., 1999, Fault transmissibility multipliers for flow simulation models: Petroleum Geoscience, v. 5, p. 53–63.
Manzocchi, T., Carter, J.N., Skorstad, A., Fjellvoll, B., Stephen, K.D., Howell, J.A., Matthews, J.D., Walsh, J.J., Nepveu, M., Bos, C., Cole, J., Egberts, P., Flint, S., Hern, C., Holden, L., Hovland, H., Jackson, H., Kolbjørnsen, O., MacDonald, A., Nell, P.A.R., Onyeagoro, K., Strand, J., Syversveen, A.R., Tchistiakov, A., Yang, C., Yielding, G., and Zimmerman, R., 2008a, Sensitivity of the impact of geological uncertainty on production from faulted and unfaulted shallow marine oil reservoirs—objectives and methods: Petroleum Geoscience, v. 14, p. 3–15.
Manzocchi, T., Heath, A.E., Palananthakumar, B., Childs, C., and Walsh, J.J., 2008b, Faults in conventional flow simulation models: A consideration of representational assumptions and geological uncertainties: Petroleum Geoscience, v. 14, p. 91–110.
Manzocchi, T., Childs, C., and Walsh, J.J., 2010, Faults and fault properties in hydrocarbon flow models: Geofluids, v. 10, p. 94–113.
Misi, A., Iyer, S.S.S., Coelho, C.E.S., Tassinari, C.C.G., Franca-Rocha, W.J.S., Cunha, I.D.A., Gomes, A.S.R., de Oliveira, T.F., Teixeira, J.B.G., and Filho, V.M.C., 2005, Sediment hosted lead-zinc deposits of the Neoproterozoic Bambuí Group and correlative sequences, São Francisco craton, Brazil: A review and a possible metallogenic evolution model: Ore Geology Reviews, v. 26, p. 263–304.
Mouslopoulou, V., Walsh, J.J., and Nicol, A., 2009, Fault displacement rates on a range of timescales: Earth and Planetary Science Letters, v. 278, p. 186–197.
Muchez, P., Heijlen, W., Banks, D., Blundell, D., Boni, M., and Grandia, F., 2005, Extensional tectonics and the timing and formation of basin-hosted deposits in Europe: Ore Geology Reviews, v. 27, p. 241–267.
Muir-Wood, R., and King, G.C.P., 1993, Hydrological signatures of earthquake strain: Journal of Geophysical Research, v. 98, p. 22,035–22,068.
Nelson, R., 2001, Geologic analysis of naturally fractured reservoirs: Boston, Gulf Professional Publishing, 352 p.
Neuman, S.P., 2008, Multiscale relationships between fracture length, aperture, density and permeability: Geophysical Research Letters, v. 35, L22402, doi: 10.1029/2008GL035622.

Newhouse, W.H., 1942, Structural features associated with the ore deposits described in this volume, *in* Newhouse, W.H., ed., Ore deposits as related to structural features: New Jersey, Princeton University Press, p. 9–53.

Nicol, A., Childs, C., Walsh, J.J., and Schafer, K., 2013, A geometric model for the formation of deformation band clusters: Journal of Structural Geology, v. 55, p. 21–33.

Nordgård Bolås, H.M., and Hermanrud, C., 2003, Hydrocarbon leakage processes and trap retention capacities offshore Norway: Petroleum Geoscience, v. 9, p. 321–332.

Odling, N.E., Gillespie, P., Bourgine, B., Castaing, C., Chilés, J.-P., Christensen, N.P., Fillion, E., Genter, A., Olsen, C., Thrane, L., Trice, R., Aarseth, E., Walsh, J.J., and Watterson, J., 1999, Variations in fracture system geometry and their implications for fluid flow in fractured hydrocarbon reservoirs: Petroleum Geoscience, v. 5, p. 374–384.

Osborne, M.J., and Swarbrick, S.E., 1998, Mechanisms for generating overpressure in sedimentary basins: A revaluation: AAPG Bulletin, v. 81, p. 1023–1041.

Peacock, D.C.P., and Sanderson, D.J., 1991, Displacements, segment linkage and relay ramps in normal fault zones: Journal of Structural Geology, v. 13, p. 721–733.

Phillips, W.J., 1972, Hydraulic fracturing and mineralization: Journal of the Geological Society, London, v. 8, p. 337–359.

Pickup, G.E., Ringrose, P.S., Corbett, P.W.M., Jensen, J.L., and Sorbie, K.S., 1995, Geology, geometry and effective flow: Petroleum Geoscience, v. 1, p. 37–42.

Pirajno, F., 2000, Indirect links: Sedimentary rock-hosted ore deposits. Epilogue, *in* Pirajno, F., ed., Ore deposits and mantle plumes: Dordrecht, Springer, 557 p.

Roberts, A., and Yielding, G., 1994, Continental extensional tectonics, *in* Hancock, P., ed., Continental deformation: Oxford, Pergamon Press, p. 223–250.

Rowe, J., and Burley, S.D., 1997, Faulting and porosity modification in the Sherwood Sandstone at Alderley Edge, northeastern Cheshire: An exhumed example of fault-related diagenesis: Geological Society, London, Special Publication 124, p. 325–352.

Rudnicki, J.W., and Chen, C.-H., 1988, Stabilization of rapid frictional slip on a weakening fault by dilatant hardening: Journal of Geophysical Research, v. 93, p. 4745–4757.

Secor, D.T., 1965, Role of fluid pressure in jointing: American Journal of Science, v. 263, p. 633–646.

Seebeck, H., Nicol, A., Walsh, J.J., Childs, C., Beetham, R.D., and Pettinga, J., 2014, Fluid flow in fault zones from an active rift: Journal of Structural Geology, v. 62, p. 52–64.

Selley, D., Broughton, D., Scott, R.J., Hitzman, M., Bull, S.W., Large, R.R., McGoldrick, P.J., Croaker, M., and Pollington, N., 2005, A new look at the geology of the Zambian Copperbelt: Economic Geology 100th Anniversary Volume, p. 965–1000.

Sevastopulo, G.D., and Redmond, P., 1999, Age of mineralization of carbonate-hosted, base metal deposits in the Rathdowney Trend, Ireland: Geological Society, London, Special Publication 155, p. 303–311.

Sibson, R.H., 1987, Earthquake rupturing as a mineralizing agent in hydrothermal systems: Geology, v. 15, p. 701–704.

——1990, Conditions for fault valve behavior: Geological Society, London, Special Publication 54, p. 15–28.

——1992, Implications of fault-valve behaviour for rupture nucleation and recurrence: Tectonophysics, v. 211, p. 283–293.

——1996, Structural permeability of fluid-driven fault-fracture meshes: Journal of Structural Geology, v. 18, p. 1031–1042.

——2000, Fluid involvement in normal faulting: Journal of Geodynamics, v. 29, p. 469–499.

——2001, Seismogenic framework for hydrothermal transport and ore deposition: Reviews in Economic Geology, v. 14, p. 25–50.

Sibson, R.H., and Scott, J., 1998, Stress/fault controls on the containment and release of overpressured fluids: Examples from gold-quartz vein systems in Juneau, Alaska; Victoria, Australia and Otago, New Zealand: Ore Geology Reviews, v. 13, p. 293–306.

Sibson, R.H., Moore, J.M.M., and Rankin, A.H., 1975, Seismic pumping—a hydrothermal fluid transport mechanism: Journal of the Geological Society, London, v. 131, p. 653–659.

Stein, R.S., and Barrientos, S.E., 1985, Planar high-angle faulting in the Basin and Range: Geodetic analysis of the 1983 Borah Peak, Idaho, earthquake: Journal of Geophysical Research, v. 90, p. 11,355–11,366.

Swarbrick, R.E., Osborne, M.J., and Yardley, G.S., 2002, Comparison of overpressure magnitude resulting from the main generating mechanisms: AAPG Memoir, v. 76, p. 1–12.

Taylor, S., 1984, Structural and paleotopographic controls of lead-zinc mineralization in the Silvermines orebodies, Republic of Ireland: Economic Geology, v. 79, p. 529–548.

Torremans, K., Kyne, R., Doyle, R., Güven, J., and Walsh, J., 2017, Structurally controlled fluid flow pathways in the Irish Zn-Pb ore field: Insights from metal distributions at the Lisheen and Silvermines deposits: Society for Geology Applied to Mineral Deposits, 14th Biennial SGA Meeting, Quebéc City, Canada, August 20–23, 2017, Proceedings, p. 641–644.

Turner, R.J.W., 1990, Jason stratiform Zn-Pb-barite deposit, Selwyn Basin, Canada (NTS 105-0-1): Geological setting, hydrothermal facies and genesis: Geological Survey of Canada, Open File 2169, p. 137–175.

van der Zee, W., and Urai, J.L., 2005, Processes of normal fault evolution in a siliciclastic sequence: A case study from Miri, Sarawak, Malaysia: Journal of Structural Geology, v. 27, p. 2281–2300.

Wallace, R.E., 1987, Grouping and migration of surface faulting and variations in slip rates on faults in the Great Basin province: Bulletin of the Seismological Society of America, v. 77, p. 868–876.

Walsh, J.J., and Watterson, J., 1988, Analysis of the relationship between displacements and dimensions of faults: Journal of Structural Geology, v. 10, p. 239–247.

——1991, Geometric and kinematic coherence and scale effects in normal fault systems: Geological Society, London, Special Publication 56, p. 193–203.

Walsh, J.J., Watterson, J., and Yielding, G., 1991, The importance of small-scale faulting in regional extension: Nature, v. 351, p. 391–393.

Walsh, J.J., Watterson, J., Heath, A.E., and Childs, C., 1998, Representation and scaling of faults in fluid flow models: Petroleum Geoscience, v. 4, p. 241–251.

Walsh, J.J., Watterson, J., Bailey, W.R., and Childs, C., 1999, Fault relays, bends and branch-lines: Journal of Structural Geology, v. 21, p. 1019–1026.

Wells, D.L., and Coppersmith, K.J., 1994, New empirical relationships among magnitude, rupture length, rupture width, rupture area, and surface displacement: Bulletin of the Seismological Society of America, v. 84, p. 974–1002.

Wibberley, C.A.J., Yielding, G., and Di Toro, G., 2008, Recent advances in the understanding of fault zone internal structure: A review: Geological Society, London, Special Publication 299, p. 5–33.

Wilkins, S.J., and Naruk, S.J., 2007, Quantitative analysis of slip-induced dilation with application to fault seal: AAPG Bulletin, v. 91, p. 97–113.

Wilkinson, J.J., 2003, On diagenesis, dolomitisation and mineralisation in the Irish Zn-Pb orefield: Mineralium Deposita, v. 38, p. 968–983.

——2010, A review of fluid inclusion constraints on mineralization in the Irish ore field and implications for the genesis of sediment-hosted Zn-Pb deposits: Economic Geology, v. 105, p. 417–442.

——2014, Sediment-hosted zinc-lead mineralization, *in* Holland, H., and Turekian, K., eds., Treatise on geochemistry 13: Oxford, Elsevier, p. 219–249.

Wilkinson, J.J., and Hitzman, M.W., 2015, The Irish Zn-Pb orefield: The view from 2014, *in* Archibald, S.M., and Piercey, S.J., eds., Current perspectives on zinc deposits: Dublin, Irish Association for Economic Geology, p. 59–72.

Wilkinson, J.J., Eyre, S.L., and Boyce, A.J., 2005, Ore-forming processes in Irish-type carbonate-hosted Zn-Pb deposits: Evidence from mineralogy, chemistry, and isotopic composition of sulfides at the Lisheen mine: Economic Geology, v. 100, p. 63–86.

Wilkinson, J.J., Crowther, H.L., and Coles, B.J., 2011, Chemical mass transfer during hydrothermal alteration of carbonates: Controls of seafloor subsidence, sedimentation and Zn-Pb mineralization in the Irish Carboniferous: Chemical Geology, v. 289, p. 55–75.

Yielding, G., Walsh, J.J., and Watterson, J., 1992, The prediction of small-scale faulting in reservoirs: First Break, v. 10, p. 449–460.

Yielding, G., Freeman, B., and Needham, D.T, 1997, Quantitative fault seal prediction: AAPG Bulletin, v. 81, p. 897–917.

Yielding, G., Bretan, P., and Freeman, B., 2010, Fault seal calibration: A brief review: Geological Society, London, Special Publication 347, p. 243–255.

Zhang, X., and Sanderson, D., 1996, Numerical modelling of the effects of fault slip on fluid flow around extensional faults: Journal of Structural Geology, v. 18, p. 109–119.